N-Substituted Acridinium as a Multi-Responsive Recognition Unit in Supramolecular Chemistry

Henri-Pierre Jacquot de Rouville, Johnny Hu, Valérie Heitz

N-Substituted Acridinium as a Multi-Responsive Recognition Unit in Supramolecular Chemistry

Henri-Pierre Jacquot de Rouville,* Johnny Hu, and Valérie Heitz*[a]

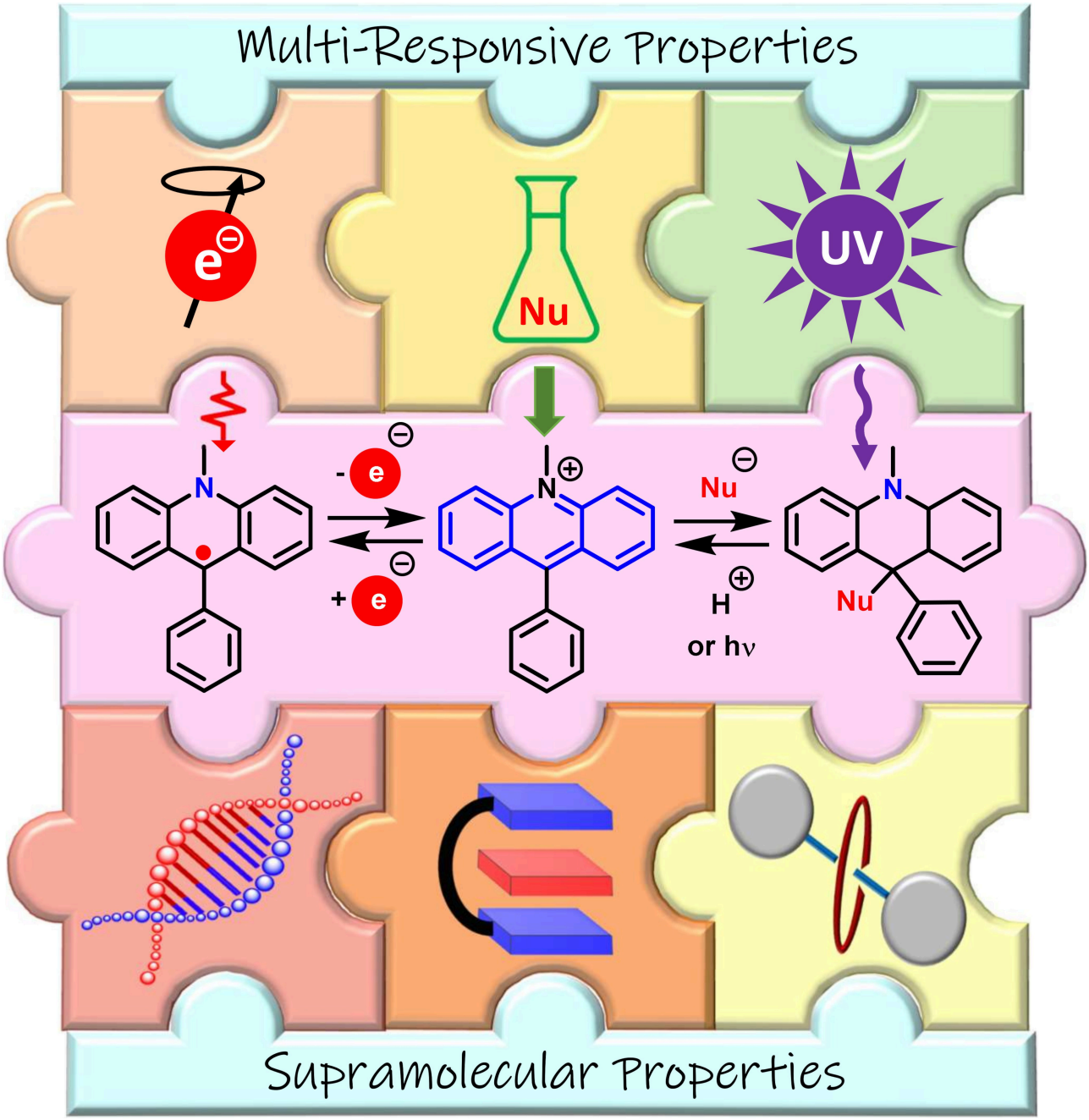

The N-substituted acridinium motif is an electron-deficient unit with appealing multi-responsive properties which have been exploited in the field of supramolecular chemistry. This building block reversibly alters its shape, and chemical and optical properties in response to a chemical or redox signal. In this Review, we discuss selected examples where the switchable properties of 9-aryl-N-methyl-acridinium lead to actuators, multi-input and multi-output systems, host or guest systems, and to interlocked systems with controllable motion.

1. Introduction

Supramolecular chemistry includes the seeking of molecular entities promoting guest binding and experiencing large and reversible geometrical, electronic, redox or luminescence modifications upon a chemical, redox or photonic stimulus. The chemical structure of these molecular entities should be easily functionalized for their incorporation in various types of architectures thus opening the way to functional devices such as guest sensors, controlled molecular drug delivery, artificial molecular machines, molecular-scale logic gates, and functional supramolecular biomaterials.[1]

The N-substituted acridinium motif represents an appealing molecular building block satisfying these requirements. It can be derivatized at both 9- and N-positions from an acridone on account of its available lone pair and ketone functional group.[2] These functionalizations allow a fine tuning of the acridinium physico-chemical properties. Especially, the 9-aryl-*N*-methyl-acridinium (**ArAc$^+$**) motif is known to exhibit multi-responsive properties relying on two extreme resonance structures. As depicted in Scheme 1 for the 9-phenylacridinium moiety (**PhAc$^+$**), on the resonance form on the right, a tritylium motif suggests halochromic and photochromic properties in an analogous way to pH-indicators (malachite green, phenolphthalein, bromothymol blue, etc.). On the resonance form on the left, a *N*-pyridinium core underlines a potential redox property.

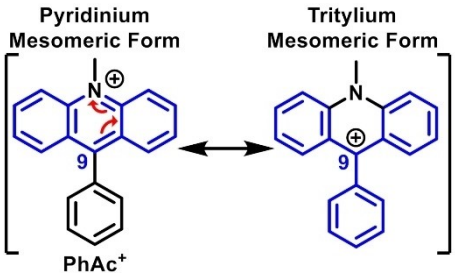

Scheme 1. Representation of two extreme resonance forms of the 9-phenyl-*N*-methyl-acridinium (**PhAc$^+$**) motif.

[a] *Dr. H.-P. Jacquot de Rouville, J. Hu, Prof. V. Heitz*
Laboratoire de Synthèse des Assemblages Moléculaires Multifonctionnels
Institut de Chimie de Strasbourg, CNRS UMR 7177
Université de Strasbourg
4, rue Blaise Pascal, 67000 Strasbourg (France)
E-mail: hpjacquot@unistra.fr
v.heitz@unistra.fr

This article is part of a Special Collection on "Supramolecular Chemistry: Young Talents and their Mentors". More articles can be found under https://onlinelibrary.wiley.com/doi/toc/10.1002/(ISSN)2192-6506.SupramolecularChemistry.

As a result of its chemio-, photo- and electrochromic properties, the **ArAc$^+$** motif has been incorporated in various supramolecular structure as a responsive unit. The scope of this review will focus on N-functionalized acridiniums with particular attention to the **ArAc$^+$** motif. Consequently, protonated acridine moieties will not be discussed in detail. A general overview on the physico-chemical properties of the acridinium core will first be discussed (section 2). The incorporation of acridinium derivatives in supramolecular systems through literature examples will then be reported. Indeed, acridinium moieties acting as guests (section 3) and as hosts (section 4) will be examined. Finally, mechanically interlocked molecules with acridinium units as component of the ring or of the dumbbell will be presented (section 5).

2. Physico-Chemical Properties

2.1. Absorption and Emission Properties

The **PhAc$^+$** molecule exhibits typical absorption bands including three vibroelectronic maxima at 451 ($\varepsilon = 3.600$ mol L^{-1} cm^{-1}), 426 (5.600), and 408 nm (5.000) for the ^1L_a transition and two maxima at 362 (18.900) and 342 nm (8.900) for the ^1L_b transition (Figure 1).[3,4]

The fluorescence properties strongly depend on the nature of the functional group at the 9-position.[5,6] Introduction of a proton or a methyl leads to high emission quantum yield ($\lambda_{em} =$ 490 nm, $\Phi \sim 1$, $\tau \sim 35$ ns, CH_3CN) whereas introduction of a phenyl leads to lower quantum yield ($\lambda_{em} = 510$ nm, $\Phi \sim 0.06$, $\tau \approx 1$ ns, CH_3CN) as the result of non-radiative relaxation pathways and competitive photo-induced electron transfer from the phenyl to the acridinium core. Noteworthy, the shift of the

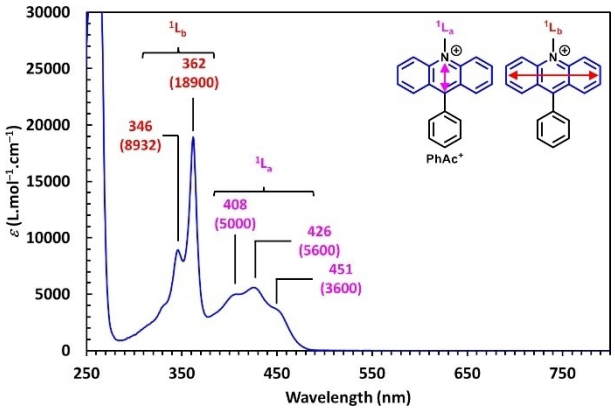

Figure 1. UV-Vis spectrum (CH_3CN, 298 K) of **PhAc$^+$**. (Data from the Supporting Information of reference [4] in accordance with reference [3]).

emission is evidence of the partial charge transfer from the phenyl to the acridinium moiety.

The emission band can be further red-shifted if the phenyl at the 9-position is functionalized by aromatic donors due to the migration of the electron density from the donor to the acridinium core (up to $\lambda_{em} = 680$ nm for 9-(4-aminophenyl) acridinium). This shift is accompanied by a fluorescence decrease ($\phi < 0.001$) resulting from an electron transfer from the donor to the excited acridinium core followed by a fast charge recombination. Noteworthy, these properties were judiciously exploited in photocatalysis as shown in various articles in the literature.[7]

2.2. Chemiochromic and Photochromic Properties

The carbocation **ArAc$^+$** undergoes the addition of nucleophiles at the 9-position, even weak ones, showing that the predominant form is the tritylium resonance motif. In alcoholic solutions (CH_3OH, ethanol, 2-propanol, *tert*-butanol, 1-pentanol), the chemical conversion of the 9-phenylacridinium (**PhAc$^+$**) to its corresponding alkoxyacridane form (**PhAcOR**) is observed in the presence of a base K_2CO_3 (Figure 2a).[8] The UV-Vis spectrum shows a clear hypsochromic shift of the electronic transitions witnessing the dearomatization of the acridinium core ($\lambda_{max} =$ 320 nm ($\varepsilon = 3800$ mol L^{-1} cm^{-1}) and 280 nm (19000) in CH_3OH).[3] In alcoholic solutions, the rate constant of the reaction is dependent on the bulkiness of the alcohol used ($CH_3OH >$ $CH_3CH_2OH >$ 2-propanol > *tert*-butanol). Interestingly in CH_3OH, the formed **PhAcOMe** reaches a stationary state (alkoxyacridane/acridinium 63:37, $K_D = 5000$ mol L^{-1}). Upon heating the methanolic solution, the observed equilibrium was shifted to the acridinium form witnessing the weak C–O bond in the alkoxyacridane moiety. The equilibrium is dependent on the solvent. In CH_3CN, this equilibrium strongly shifts to the **PhAcOR** form (98%, $K_D = 9$ mol L^{-1}). Indeed, CH_3CN is less polar than CH_3OH thus destabilizing the positively charged acridinium moiety. In all solvents, restoration of the acridinium form occurs upon addition of acids (even weak).

Formation of the hydroxy-acridane (**PhAcOH**) moiety is reached

upon addition of hydroxide anions. The **PhAcOH** motif exhibits the analogous halochromic properties than the **PhAcOR** motif in terms of electronic transitions, luminescent properties and chemical reactivity. Based on these properties, a scarce example of a regenerable chemodosimeter of oxophilic metal cations was provided by T. C. Sutherland and his group (Figure 2b).[9] Oxophilic metal cations (Al^{3+}, In^{3+} and Zn^{2+}) were added to the **PhAcOH** moiety in CH_3CN resulting in a red-shift of the electronic transitions in absorption (λ_{max} from 286 nm to 424 nm) and in emission (from $\lambda_{em} = 348$ nm; $\phi = 0.05$ to $\lambda_{max} =$ 500 nm; $\phi = 0.05$). Metal binding led to color changes of the solutions visible in ambient light (Figure 2c). These physicochemical changes correspond to the conversion of the **PhAcOH** to the **PhAc$^+$** cation. Noteworthy, this conversion does not occur in the presence of alkali metal cations such as Li^+, Na^+ and TBA^+ cations.

Light is an alternative stimulus to acids for the restoration of the **PhAc$^+$** aromaticity from an acridane moiety (Scheme 2).[3] Irradiation of acridane units leads to the heterolytic photodissociation of the C–O bond at the 9-position of the acridane core ($\lambda_{max} \approx 280$ nm) and to an increase in absorbance in the

Johnny Hu received his Master's Degree from the University of Strasbourg in Molecular and Supramolecular Chemistry. In 2019, he started his PhD under the supervision of Prof. Valérie Heitz and Dr. Henri-Pierre Jacquot de Rouville. His work focuses on the synthesis of new switchable receptors including acridinium moieties as recognition units.
I am thankful to Valérie and Henri-Pierre for their support and expertise during my PhD thus giving me the opportunity to work on supramolecular systems. I am glad to contribute to this Special Collection with this Review dedicated to acridinium units and their role as multi-responsive recognition unit in supramolecular systems.

Henri-Pierre Jacquot de Rouville graduated from the Université Paul Sabatier, Toulouse. In 2007, he joined C. Joachim's Group and obtained a PhD degree for his synthesis of technomimetic molecules for nanomechanical applications under the supervision of Professor G. Rapenne (CEMES-CNRS, Toulouse). From 2010 to 2012, he worked in Professor J. F. Stoddart's group as a postdoctoral fellow where he investigated the chemistry of mechanically interlocked molecules. Then, he moved back to France where he worked as a postdoctoral fellow with N. McClenaghan (ISM, Bordeaux). In 2013, he was appointed as Chargé de Recherche (full time researcher at the CNRS) at the laboratory ITODYS, Paris. In November 2017, he moved at the Institut de Chimie in Strasbourg where he joined the LSAMM research group.

Valérie Heitz is a Professor in Chemistry at the University of Strasbourg and the head of the Laboratory of Synthesis of Multifunctional Molecular Assemblies (LSAMM). She obtained a Ph.D in 1992 in the field of artificial photosynthesis under the supervision of Dr. J.-P. Sauvage. After postdoctoral work with Prof. A. Harriman (University of Texas at Austin), she obtained an assistant professor position in the group of Dr. J.-P. Sauvage. She was involved in many projects in the field of mechanically interlocked compounds as artificial molecular machines. She started her own group in 2010 and her current interests are in functional dynamic systems, supramolecular architectures incorporating porphyrins, molecular machines, and bifunctional systems for theranostic applications.

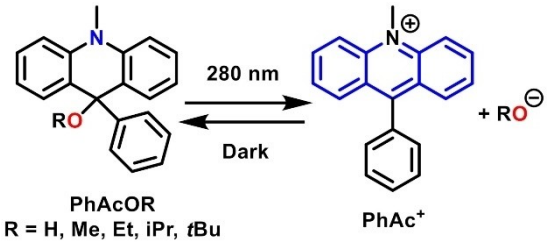

Scheme 2. Photochromic properties of the acridane (**PhAcOH** and **PhAcOR**) moieties. Photoconversion to the acridinium form occurs upon irradiation at 280 nm in polar solvents.[3]

visible region ($340 < \lambda < 450$ nm) in agreement with the formation of the corresponding **PhAc$^+$**. As in the halochromic studies, the acridinium-acridane photo-stationary state is solvent dependent (44:56 in CH_3OH, 45:55 in CH_3CH_2OH, 49:51 in 2-propanol and 17:83 in CH_3CN).

The photoconversion of a solution of **PhAcOH** and **PhAcOMe** in a CH_3CN/H_2O (2:1) solvent mixture was also followed by ^1H NMR spectroscopy by the group of J. Fréchet.[10] Upon irradiation at 280 nm, heterolytic bond cleavage of the hydroxide and methoxide anions was confirmed by the downfield shifts of all proton signals. These shifts clearly indicate the restoration of the **PhAc$^+$** aromaticity. In addition, the photoejection of the hydroxide and methoxide anions led to an increase of the pH of the solution. Interestingly, the back reaction was found to be slower for the acridinium fragment than for malachite green under similar conditions. This observation suggests that the **PhAc$^+$** is more stable than malachite green on account of its polyaromatic character, in agreement with their respective equilibrium conversion constants ($pK_R^+ = 11.03$ and $pK_R^+ = 6.94$).[11] It underlines the importance of the nature of the cation in the recombination process.

Investigation of the excited-state dynamics of **PhAcOR** moiety (R-=H- and CH_3-) using femtosecond (fs) and nanosecond (ns) transient absorption (TA) spectroscopy was performed by the group of K. D. Glusac (Figure 3).[12] This investigation confirmed the importance of the solvent in the heterolytic bond cleavage. In protic solvents, such as CH_3OH, the first excited singlet state (S_1) has a relatively long lifetime ($\tau = 108$ ps) allowing the formation of **PhAc$^+$**. In comparison, aprotic solvents (such as CH_3CN and benzene) gave rise to a more complex mechanism involving an intersystem crossing populating the first triplet state (T_1). The authors postulated that the absence of C–O bond cleavage from this T_1 state is due to a conical intersection with the S_0 state that restores the **PhAcOH** ground state.

The influence of the substituent (-CN < -CF_3 < -H < -OH < -NMe_2) at the *para* position of the phenyl ring of **PhAcOH** and the influence of the solvent polarity ($H_2O < CH_3OH <$ n-BuOH < i-BuOH) on the photoreactivity of the acridane core was also demonstrated.[13] This observation can be rationalized by the stabilization of the positive charge of the acridinium species by electron donating functional groups and by polar solvents. This behavior was evidenced by the rate constant decay of the acridane S_1 state increasing upon increasing the electron donating nature of the functional group.

Spiro-acridanes are acridane systems whose nucleophile leads to an intramolecular addition.[14] A series of spiro-acridane were prepared by W. Abraham and coworkers incorporating an

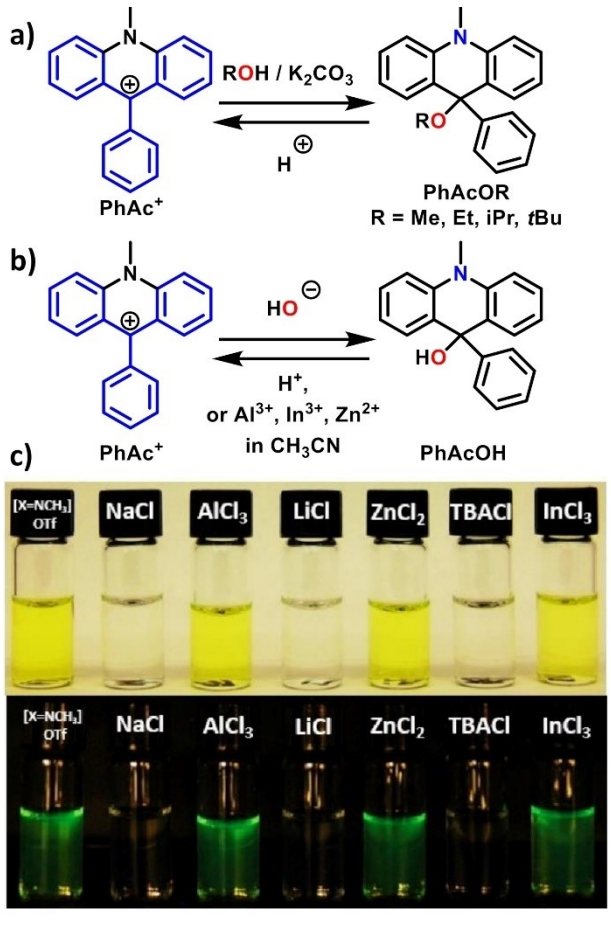

Figure 2. Chemiochromic properties of the acridinium core leading to the corresponding acridane a) **PhAcOR** (R = Me, Et, iPr, *t*Bu)[8] and b) **PhAcOH** and c) color change under ambient light (top) and UV light (365 nm) that enable chemiodosimetry of oxophilic metal cations.[9] Reproduced from reference [9] with permission from Royal Society of Chemistry.

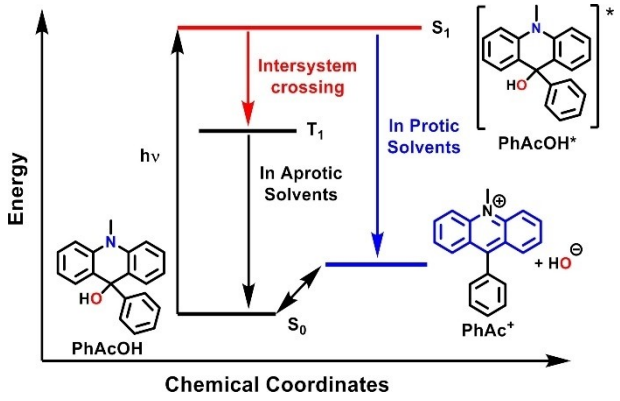

Figure 3. Schematic energetic diagram explaining the photochemical behavior of the hydroxy-acridane moiety in aprotic (benzene, acetonitrile) or protic (CH_3OH) solvents.[12] Reproduced from reference [12] with permission from the American Chemical Society.

alcohol on the phenyl at the 9 position (**1**) (Scheme 3).[15] Upon irradiation in CH_3OH, a ring opening takes place thus revealing an **Ac**$^+$ core. Stability of the charged species was governed by the size of the ring of the spiro-acridanes. Formation of 5-membered rings was found to be faster than 6-membered rings with respective lifetimes of 0.007 and 13 seconds.

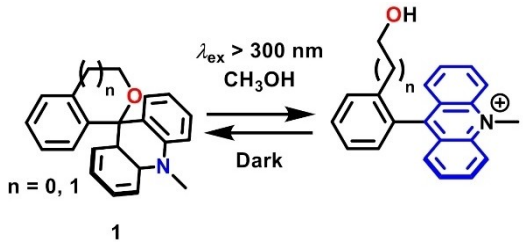

Scheme 3. Spiro-acridane systems (**1**) developed by the group of W. Abraham.[15]

2.3. Electrochemical Properties

The acridinium core can be considered as an extended pyridinium core. In comparison to the pyridinium core, the extension of the π-system of the acridinium moiety lowers the reduction potential of the first and second reduction wave on account of the decrease of the LUMO energy. Indeed, the **PhAc**$^+$ cation exhibits a reversible reduction wave in CH_3CN ($E_1 = -0.54$ V *vs* SCE)[16a] as well as in DMF and in DMSO (Figure 4a).[16b] Spectroelectrochemistry shows stability of the acridine radical for days if kept under argon. Further reduction leads to an irreversible second reduction wave ($E_2 = -1.48$ V *vs* SCE)[16a] resulting in a carbanionic species able to deprotonate solvent molecules.[16c] This observation was corroborated by a drop in the anodic current of the re-oxidation peak. This behavior is typical of the formation of a new species according to an EEC (Electron Electron Chemical) mechanism (Figure 4). Noteworthy, reduction of parent acridinium (**Ac**$^+$) leads to an irreversible reduction wave ($E = -0.54$ V vs SCE) as the result of the dimerization of the **Ac**$^\bullet$ radical (Figure 4b). Subsequent oxidation of the dimer leads to lucigenin, a tail-to-tail acridinium dimer.[16a,d] Thus, introduction of a phenyl at the 9-position prevents the dimer formation leading to a reversible reduction wave.

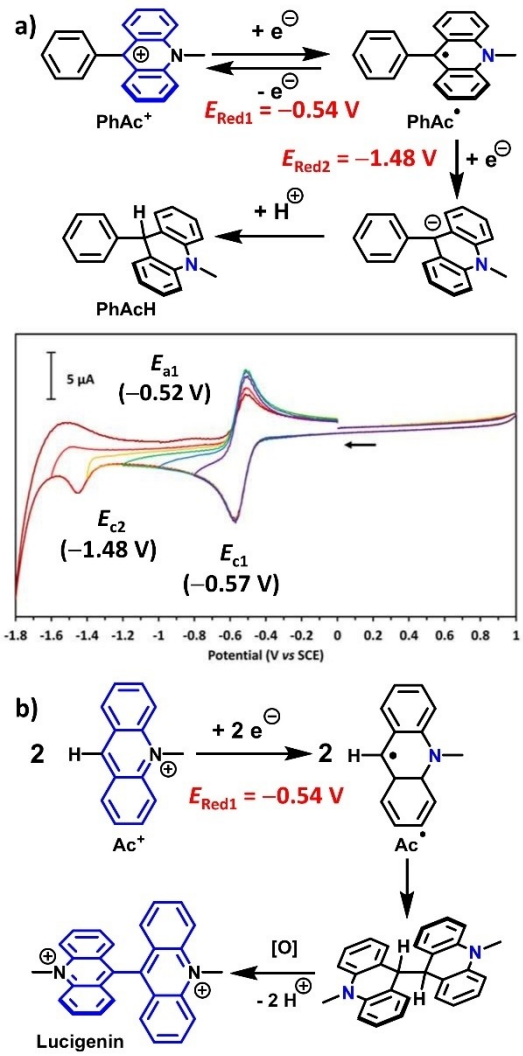

Figure 4. a) EEC mechanism upon reduction of the **PhAc**$^+$ motif leading to the formation of the **PhAcH** moiety (personal ■ Unpublished? ■ data consistent with reported systems ■ OK? ■).[16] b) EC mechanism of **Ac**$^+$ leading to lucigenin.[17]

As seen with the formation of lucigenin,[17] redox properties of **Ac**$^+$ are tuned according to the functional group at the 9-position of the acridinium core. Similarly, introduction of a dimesitylborane functional group shifts the cathodic waves to more positive potentials.[18]

2.4. Electrochemical Actuators

The electrochemical properties of the acridinium units were exploited to develop a series of electrochemical actuators (named as *dynamic redox* systems or *dyrex* systems) by the group of T. Suzuki (Figure 5). First reported in 1997, this family of molecules incorporated tritylium electroactive moieties.[19] In 2003, a 2,2′-biphenyl scaffold functionalized with two acridiniums as redox active sites was reported (**2**$^{2+}$, Figure 5a).[20] Upon chemical reduction, an intramolecular C_{sp3}-C_{sp3} elongated bond (1.635 Å) was formed leading to the corresponding bis-acridane derivative (**2**^{0}). This elongated bond is the result of the steric repulsion existing between both acridane moieties. It can be reversibly formed and cleaved either electrochemically or chemically (reduction using Zn(0) and oxidation using magic blue). Consequently, this compound exhibits an electrochemical bistability showing an electrochemical hysteresis loop with a potential difference (ΔE) of 0.45 V between the reduction ($E_{Red} = -0.27$ V *vs* SCE) and the oxidation peaks ($E_{Ox} = +0.18$ V *vs* SCE). Interestingly, this redox switch also gave rise to optical responses from yellow colored and green emissive for the oxidized form to colorless and non-emissive for the reduced form, as shown in CH_3CN. The hypsochromic shifts in the optical spectrum of the reduced species was easily rationalized by the

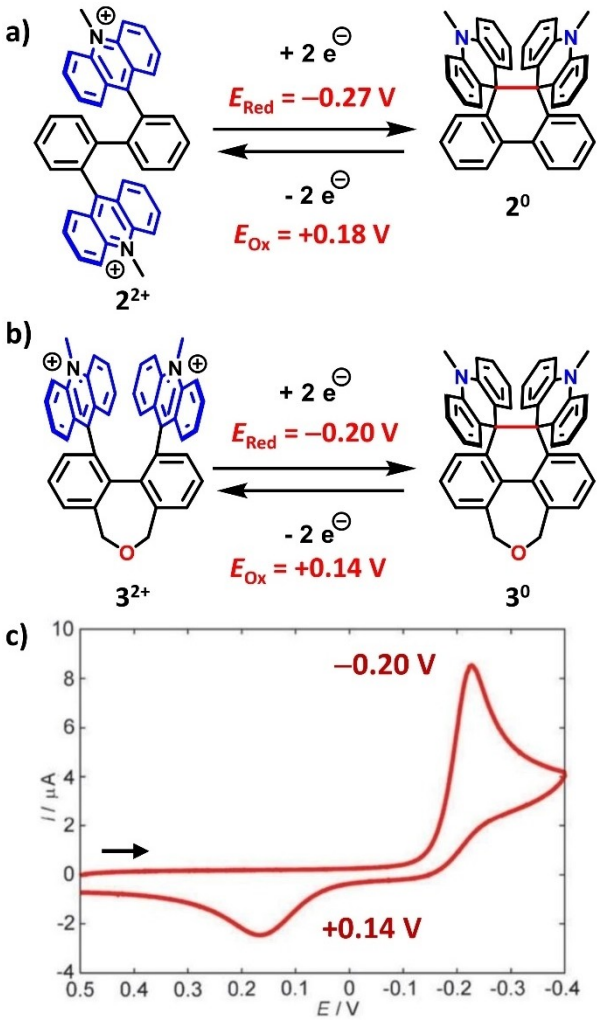

Figure 5. Dyrex systems developed by T. Suzuki built around a) a 2,2′-biphenyl ($\mathbf{2}^{2+}$)[20] and b) 5,7-dihydrodibenzo[c,e]oxepine scaffold ($\mathbf{3}^{2+}$). c) Cyclic voltammogram of $\mathbf{3}^{2+}$ Dyrex system (E/V vs. SCE, Pt electrode, scan rate 100 mV s^{-1}, 0.1 mol L^{-1} of Et_4NClO_4 in CH_3CN) showing the opening of an electrochemical hysteresis loop.[21a] Reproduced from reference [21a] with permission from Royal Society of Chemistry.

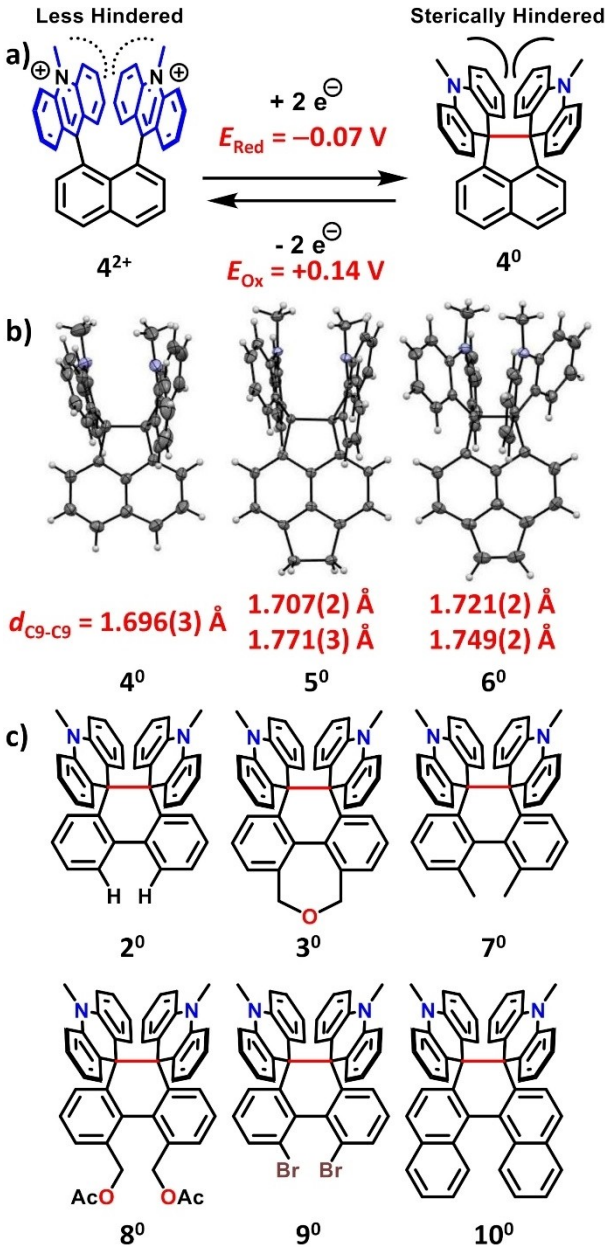

Figure 6. (a) and (b) Dyrex systems built around rigid naphthalene, acenaphthene and acenaphthylene scaffolds and the X-ray structures of the corresponding reduced forms ($\mathbf{4}^0$-$\mathbf{6}^0$).[22] Length of the C9-C9 bonds are indicated (in Å) for all the independent molecules found in the crystals. c) Dyrex systems built around semi-rigid scaffolds ($\mathbf{2}^0$, $\mathbf{3}^0$, $\mathbf{7}^0$–$\mathbf{10}^0$).[21] Reproduced from reference [22b] with permission from Wiley-VCH.

dearomatization of the acridinium units. The hysteresis properties were also modulated according to the scaffold used changing the pre-organization of the acridinium units (Figure 5b-c as an example on $\mathbf{3}^{2+}$ built around a 5,7-dihydrodibenzo[c,e]oxepine platform).[21a]

The length of the elongated bond was altered according to the spacer used. For examples, systems built on a rigid naphthalene, acenaphthene and acenaphthylene scaffolds gave rise to an increase distance between the C_9 atoms of the corresponding acridanes ($\mathbf{4}^0$), ($\mathbf{5}^0$) and ($\mathbf{6}^0$) (Figure 6a–b).[22] This behavior was rationalized by the "back-clamping" (provided by the bridging unit connecting the two aryl rings) at the *peri* position of the naphthalene scaffold thus increasing the angle strain between the redox units. In addition, the length of the elongated bond was modulated according to the functionalization of the bay region of the biphenyl scaffold at the 6,6′ positions ($\mathbf{2}^0$, $\mathbf{3}^0$, $\mathbf{7}^0$–$\mathbf{10}^0$; Figure 6c).[21]

2.5. Multi-Input and Multi-Output Responsive Systems

In addition to the exploitation of the electrochemical properties of the acridinium units, multi-state (more than two states) and multi-input / multi-output responsive systems were developed.

An example relies on the use of a 2,2′-bipyridyl spacer ($\mathbf{11}^{2+}$, Scheme 4).[23] As expected and confirmed by X-ray analysis, the acridinium units in the oxidized form adopt an *anti*-conformation on account of the nitrogen atoms lone pair repulsion, the charge repulsion and the steric hindrance between both

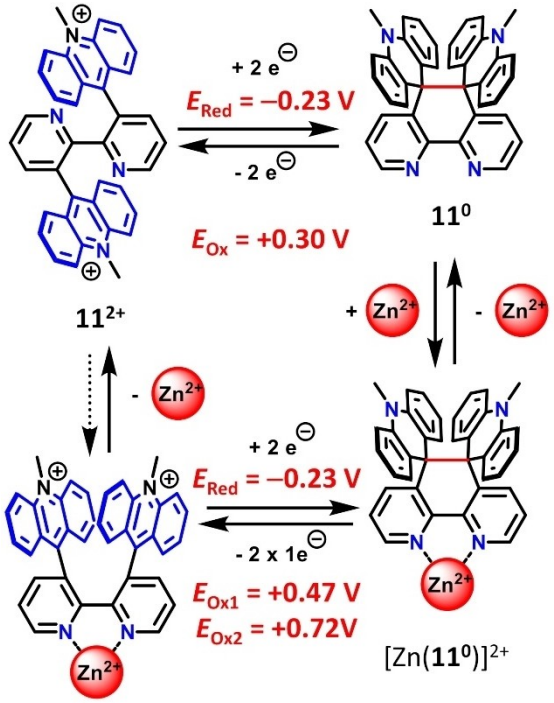

Scheme 4. Dyrex system built around a 2,2′-bipyridine scaffold ($\mathbf{11}^{2+}$) able to bind a Zn(II) cation upon reduction.[23] Reproduced from reference [23] with permission from Elsevier.

acridinium units. Upon reduction, the orientation of the two N atoms are in a *syn* conformation ($\mathbf{11}^{0}$) allowing the coordination of the Zn(II) cations $[Zn(\mathbf{11}^{0})]^{2+}$ as confirmed by ^{1}H NMR (signal spreading over the aromatic region) and UV-visible (red shift) spectroscopies. Noteworthy, formation of the Zn(II) bis-acridinium complex does not take place in the unfavored *anti* geometry. Upon complexation of Zn(II), the oxidation potential is anodically shifted and release of the Zn(II) cation occurs in a two-step oxidation process. The use of a bipyridine ligand as spacer opens to a two-way-input responsive system since Zn(II) coordination modulates also the redox properties of the *dyrex* system with two-way outputs (absorption and fluorescence).

An additional way to tune mechanical actuation of the *dyrex* system relies on the introduction of secondary/auxiliary units ($\mathbf{12}^{2+}$, Scheme 5).[24] In a first example, the helicity of the biphenyl scaffold was achieved by the N-functionalization of the acridinium by suitable chiral auxiliary centers (chiral amide groups) enabling a "chirooptical enhancement" for output signal detection. As demonstrated by ^{1}H NMR, CD-spectroscopy and FDCD studies in CH_2Cl_2, both oxidized and reduced forms exhibit a diastereomeric excess at room temperature. This diastereomeric excess was attributed to the existence of intramolecular hydrogen bonds between both chiral amide groups. Additionally, the influence of the hydrogen bonding interaction on the biphenyl scaffold twisting can be modulated according to temperature and solvent polarity. This system is a prototype of a multiresponsive system, three external stimuli (electric potential, solvent polarity, heat) being transduced into optical

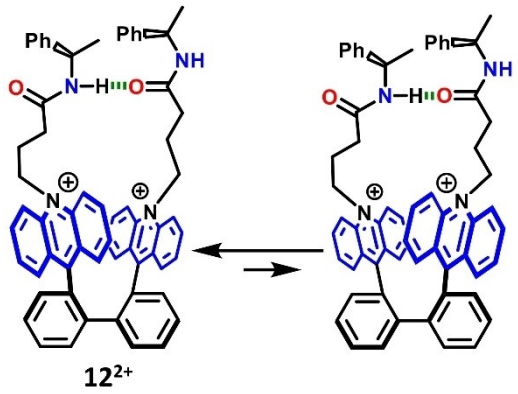

Scheme 5. Intramolecular H-bonding interactions in dyrex system ($\mathbf{12}^{2+}$) incorporating peripheral chiral amide groups for enhanced chiroptical signal.[24]

(absorption and emission) and chirooptical responses (CD and fluorescence CD).

T. Suzuki and his group have also used a dihydroxy-1,1′-biphenyl scaffold to preorganize two acridinium units ($\mathbf{13}^{2+}$, Scheme 6a).[25] As expected, this system exhibits an electrochemical hysteresis loop ($E_{Ox} = +0.32$ V and $E_{Red} = -0.23$ V *vs* SCE) in a CH_2Cl_2/CH_3CN (4:1) solvent mixture. However, the bis-acridinium form is also chemically responsive to the addition of base ($N(CH_2CH_3)_3$) leading to the formation of a dioxopyrene motif (**14**). Structural changes following dearomatization of the acridinium units were confirmed by X-ray diffraction, by hypsochromic shifts (λ_{max} from 440 to 339 nm) in UV-Vis spectroscopy and by upfield shifts of all aromatic signals in ^{1}H NMR. Under acid conditions (TfOH), the bis-acridinium precursor was restored as evidenced by the same characterization techniques.

A system involving a spiro-acridane motif was also reported in 2019 by Y. Hirao, T. Kubo and co-workers (**16**, Scheme 6b).[26] Under acidic conditions, the ring opening was monitored by UV-Vis spectroscopy thus leading to the typical spectrum of the

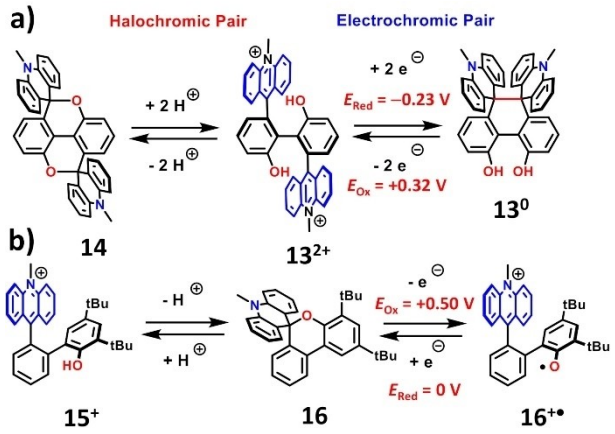

Scheme 6. Responsive acridinium systems upon chemical and electrochemical stimuli a) from T. Suzuki and co-workers ($\mathbf{13}^{2+}$)[25] and b) from T. Kubo and co-workers ($\mathbf{15}^{+}$).[26] Reproduced from reference [26] with permission from Wiley-VCH.

acridinium moiety ($\mathbf{15}^+$). The presence of isosbestic points suggests the reversibility of the ring opening process. This reversibility was further demonstrated by addition of tetrabutyl ammonium hydroxide. Electrochemical experiments showed the typical behavior of two EC mechanisms with an irreversible oxidation peak ($E_{Ox} = +0.5$ V *vs* SCE) and an irreversible reduction ($E_{Red} = 0$ V *vs* SCE). Upon oxidation, the ring opening results in the formation of a phenolic radical ($\mathbf{16}^{+\bullet}$) as confirmed by EPR. This study is a rare example of the investigation of the electrochromic properties in spiroacridanes.

3. Acridiniums as Molecular Guest

Acridinium molecules are expected to interact with themselves through π-π stacking interactions on account of their relatively large aromatic character. Their electro-deficient nature allows their involvement in π-donor/π-acceptor systems and leads to homophilic and heterophilic interactions in the solid state.[27] They also exhibited their abilities to form aggregates in micellar environments from 4-octylbenzenesulfonate and sodium lauryl sulfate.[28] Consequently, acridinium moieties were exploited in supramolecular systems acting as guests. Herein, interaction with DNA, hydrophobic hosts and π-donor receptors will be discussed.

3.1. Guest in Single Strand and Double Strand DNA

The intercalating properties of protonated acridinium derivatives are known from the sixties.[29] However, these studies did not report any binding constants. It is only in the 2000's that quantitative data of the binding of acridinium derivatives with single and double DNA were stated and were envisioned to act as a drug targeting DNA.

In vitro, complexation studies were performed by D. Ramaiah and his group between calf thymus DNA (CT DNA) and acridinium intercalators in H_2O at a pH of 7.4 (Figure 7a).[30] The binding constants of *p*-tolyl ($\mathbf{17}^+$, log $K = 4.85$) and *m*-tolyl ($\mathbf{18}^+$, log $K = 4.84$) derivatives determined from fluorescence titration were relatively close to the phenyl derivative (log $K \sim 5.04$) showing the negligible effect of the methyl on these positions of the phenyl ring in the binding event (Figure 7b). On the other hand, due to steric hindrance, negligible binding was observed with the *o*-tolylacridinium ($\mathbf{19}^+$). In addition, a preferential binding was observed for the *m*-tolyl and *p*-tolyl derivative for poly(dG)·poly(dC) than for poly(dA)·polt(dT) and CT DNA.

Interestingly, the *o*-tolyl derivative ($\mathbf{19}^+$) exhibited a binding event with the less stacked single strand DNA.[31] The intercalation of the *o*-tolyl derivative was effective for oligonucleotides containing 19 bases of same base or mixed bases with a stronger affinity for $(dC)_{19}$ (log $K = 4.48$) < $(dT)_{19}$ (4.51) < $(dA)_{19}$ (4.85) < $(dN)_{19}$ (4.88) < $(dG)_{19}$ (4.93) (Figure 8). Noteworthy, these binding constants were decreased by an order of magnitude when the ionic strength increased (from 2 mmol L^{-1} to 100 mmol L^{-1} of NaCl in H_2O) thus showing the prevalence of π-π stacking interactions over electrostatic interactions. These studies underline the possibility of these water soluble $\mathbf{ArAc}^+$ derivatives to act as fluorescent probes for various studies related to DNA structure and as a selective probe of single strand DNA over double strand DNA.

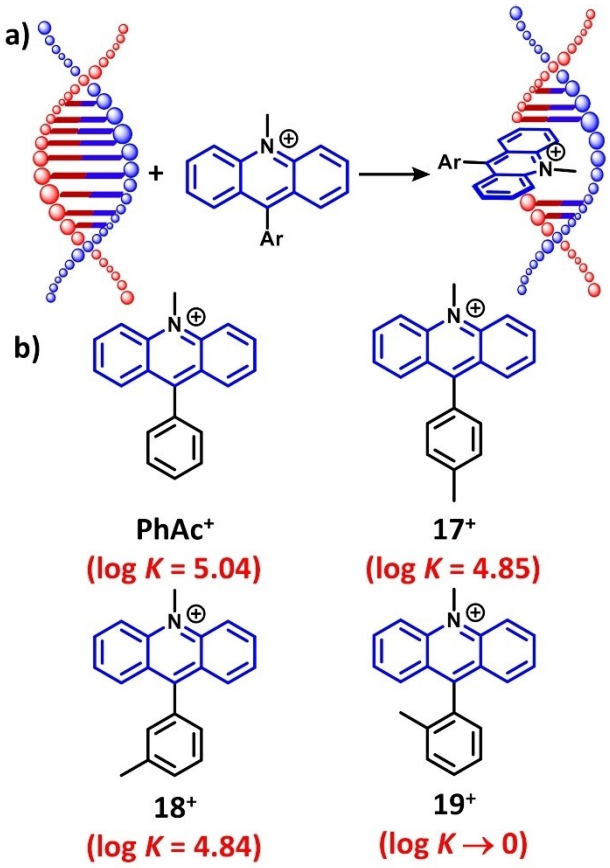

Figure 7. a) Illustration of the intercalation of $\mathbf{PhAc}^+$ and $\mathbf{17}^+$–$\mathbf{19}^+$ in double strand DNA and b) the corresponding binding constants (log *K*) in water for the different guests.[30]

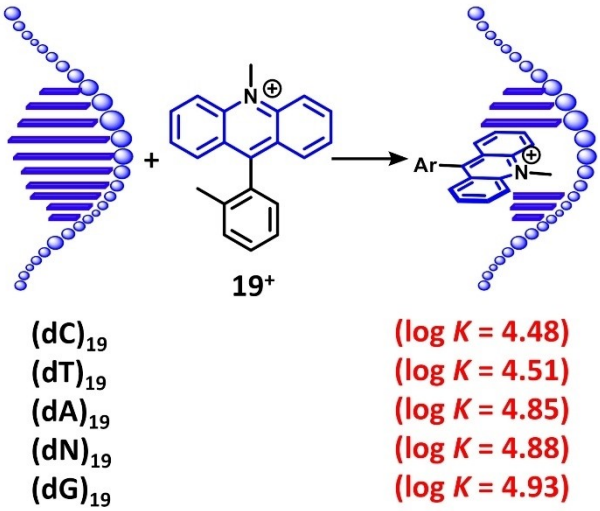

Figure 8. Illustration of the intercalation of $\mathbf{19}^+$ in single strand DNA and the corresponding binding constants (log *K*) in water for the different polynucleotides containing 19 identical bases.[31]

The same group has explored the DNA binding affinity of an acridine-acridinium derivative ($\mathbf{20}^{+}$) connected by a polymethylene spacer (Scheme 7a).[32] The acridinium moiety interacts with CT DNA (log $K = 5.67$) as attested by the observed red-shift, hypochromicity and fluorescence quenching. It was confirmed by the binding constant found for the methyl acridinium model compound which had a similar affinity (log $K = 5.86$). The fluorescence quenching was attributed to an electron transfer from DNA to the acridinium. The bis-acridinium compounds ($\mathbf{21}^{2+}$, n = 5 and $\mathbf{22}^{2+}$, n = 10) were also studied (Scheme 7b) and exhibited an increase in fluorescence quenching with the spacer length (log $K = 6.63$ for $\mathbf{21}^{2+}$ and 7.40 for $\mathbf{22}^{2+}$). These higher binding constants were confirmed by denaturation curve experiments. Indeed, the transition temperature (T_m) increased upon addition of bis-acridinium intercalators. Compared to $\mathbf{20}^{+}$, the higher binding constant for $\mathbf{21}^{2+}$ was attributed to an additional electrostatic interaction between the second acridinium moiety and the phosphate groups as demonstrated by increasing the ionic strength of the medium (from 2×10^{-3} mol L^{-1} to 0.1 mol L^{-1} of NaCl). In the case of n = 10 ($\mathbf{22}^{2+}$), the increased binding constant was the result of a bis-intercalation as reflected by viscosity experiments.

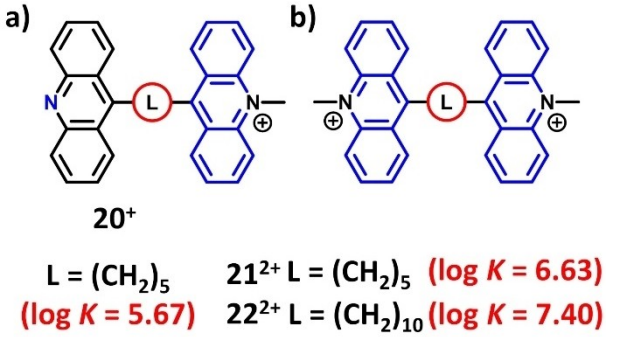

Scheme 7. a) Acridine-acridinium ($\mathbf{20}^{+}$) and b) acridinium-acridinium derivatives ($\mathbf{21}^{2+}$, n = 5 and $\mathbf{22}^{2+}$, n = 10) and the corresponding binding constants (log K) with CT DNA in water.[32]

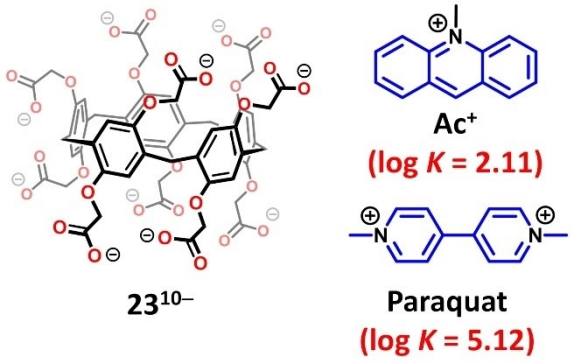

Scheme 8. Water soluble pillar[5]arene ($\mathbf{23}^{10-}$) developed by M. Xue and co-workers able to bind $\mathbf{Ac}^{+}$ and paraquat and the corresponding binding constants (log K) in water.[33]

3.2. Acridinium and Hydrophobic Interaction

M. Xue and his group have developed a fluorescent sensor for the detection of a water pollutant paraquat (Scheme 8).[33] The fluorescence sensor consists of a host-guest complex between pillar[5]arene decorated by carboxylate functional groups ($\mathbf{23}^{10-}$) and *N*-methylacridinium ($\mathbf{Ac}^{+}$) at pH 7.4. Formation of the 1:1 inclusion complex was confirmed by 1D and 2D NMR, UV-Vis and fluorescence studies. UV-Vis titration experiments allowed the estimation of the binding constant of $\mathbf{Ac}^{+}$ to be 1.28×10^{2} L mol^{-1} (log $K = 2.11$) resulting from the cooperativity between hydrophobic, π-π stacking and multiple electrostatic interactions. In addition, fluorescence quenching of the $\mathbf{Ac}^{+}$ fluorescence is observed upon complexation demonstrating the existence of a photoinduced electron transfer from the host to the guest. Displacement of the 1:1 host-guest system by competitive guest exchange with paraquat (log $K = 5.12$) leads to the release of $\mathbf{Ac}^{+}$ restoring its green emission. Noteworthy, reversible host-guest complex dissociation occurs upon acidification as a result of the precipitation of the protonated macrocycle from the aqueous medium.

Lucigenin, a fluorescent dimer of acridinium (Figure 9a) is able to interact with cucurbituril (CB[n]), a pumpkin-like receptor which has shown unprecedented binding affinities for select guest.[34] Noteworthy, the decomposition rate of lucigenin derivatives (N,N′-disubstituted-9,9′-biacridiniums $\mathbf{24}^{2+}$, $\mathbf{25}^{2+}$ and

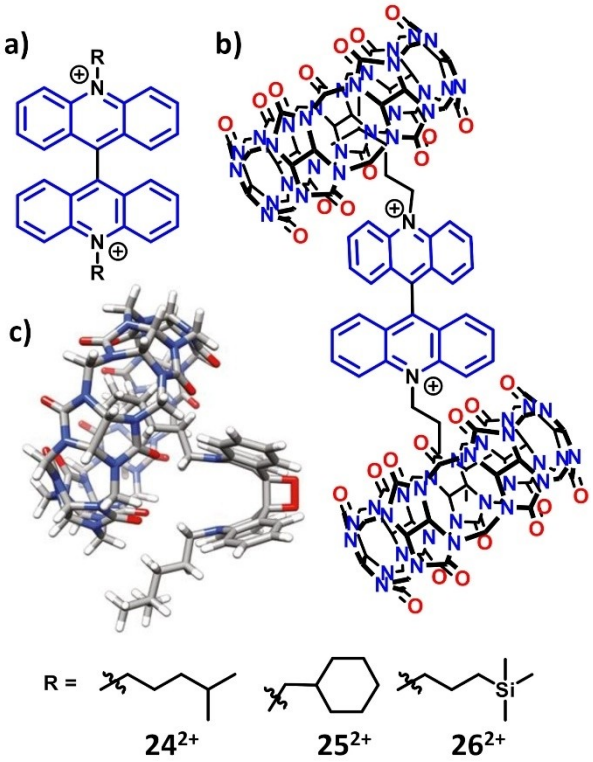

Figure 9. a) Studied lucigenins ($\mathbf{24}^{2+}$, $\mathbf{25}^{2+}$ and $\mathbf{26}^{2+}$) by the Masson group and b) a schematic representation of their complex with two CB[7] macrocycles. c) Optimized structure (PM6-D) of the dioxetane obtained by oxidation of $\mathbf{24}^{2+}$ and included in CB[7].[35] Reproduced from reference [35] with permission from the American Chemical Society.

$\mathbf{26}^{2+}$) upon addition of sodium peroxide was studied in the presence of CB[7] (Figure 9b).[35] Indeed, these lucigenins undergo an oxidative degradation leading to the emission of cyan light (λ_{max} = 485 nm; rate constants of light emission decays are 1.8×10^{-3}, 2.0×10^{-3}, and 5.8×10^{-3} s^{-1}). Upon addition of CB[7], light emission was immediately interrupted or decreased by one order of magnitude thus exhibiting the good affinity of lucigenin toward CB[7] ($5.00 < \log K < 9.23$). Indeed, encapsulation of lucigenin derivatives prevented or decreased the decomposition of the dioxetane oxidation intermediates (see Figure 9c). The light emission was restored upon addition of either xylylene or adamantylpyridinium acting as competitive guest.

The ability of $\mathbf{Ac}^+$ to be involved in π-donor/π-acceptor interactions with calixarenes was first demonstrated by S. Shinkai and his group.[36] Encapsulation of acridinium iodide salt with calix[n]arene receptors (n = 4, 5 and 8) in a face-to-face arrangement was evidenced by NMR spectroscopic techniques. The complexes were formed in relatively high affinity ($1.90 < \log K < 3.38$) in $CDCl_3/CD_3CN$ (10:2).

M. Stępień and coworkers have functionalized a calix[4]arene with a oligophenylene loop (**27**) which delimits a flexible cavity (Figure 10a).[37] Followed by NMR experiments, titration studies in CD_2Cl_2 revealed a 1:1 host-guest complex between $\mathbf{Ac}^+$ and the oligophenylene loop through π-π interactions ($\log K = 3.77$, Figure 10b). Interestingly, the 1:1 association event was preceded by the formation of a less stable 2:1 host-guest complex ($\log K = 2.63$). The affinity for $\mathbf{Ac}^+$ was the strongest among other studied acceptor guests such as neutral anthraquinone or the cationic diquat. The optical properties of the host-guest complexes were also analyzed from an amorphous thin film obtained by drop casting. Upon $\mathbf{Ac}^+$ complexation, a red-shift of the absorption band of the receptor in the visible region (λ_{max} from 380 nm to 411 nm) and a red-shift of fluorescence (λ_{max} from 500 nm to 700 nm) were monitored. In addition to the fluorescence color change, a partial quenching was observed assigned to a charge transfer from the electron rich oligophenylene loop of **27** to the $\mathbf{Ac}^+$ accepting moiety, from TD-DFT calculations.

Noteworthy, bis-porphyrin receptors interacting through π-donor/π-acceptor interactions with protonated acridine derivatives have been prepared.[38] As an example, large binding constants were determined on account of the extended π-systems of the receptors **28**–**30** (Scheme 9).[38c–e]

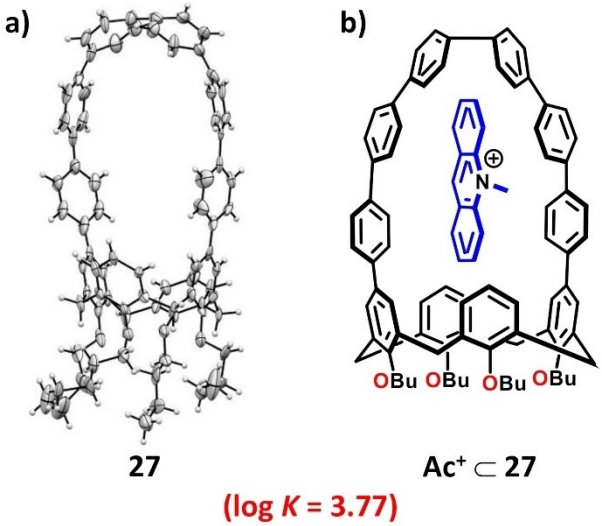

Figure 10. Functionalized calix[4]arene with a bent oligophenylene loop (**27**). a) X-ray crystal structure and b) π-π interactions with $\mathbf{Ac}^+$ with the corresponding binding constant (log *K*) in CD_2Cl_2.[37]

4. Acridiniums in Molecular Hosts

In this section, supramolecular hosts involving acridinium moieties either as signaling units appended to receptors or as recognition sites will be described.

4.1. Acridinium Appended to Macrocyclic Receptors

The complexation properties of a receptor consisting of 9-phenylacridinium linked to a 15-aza-crown recognition unit at the *para* position of the phenyl ring were reported by J. W. Verhoeven and his coworkers ($\mathbf{31}^+$, Figure 11).[39] This compound exhibited an intense charge transfer band (λ_{max} = 562 nm, $\varepsilon = 9800\ L\,mol^{-1}\,cm^{-1}$ in CH_3CN) as the result of the partial delocalization of the aniline lone pair to the acridinium

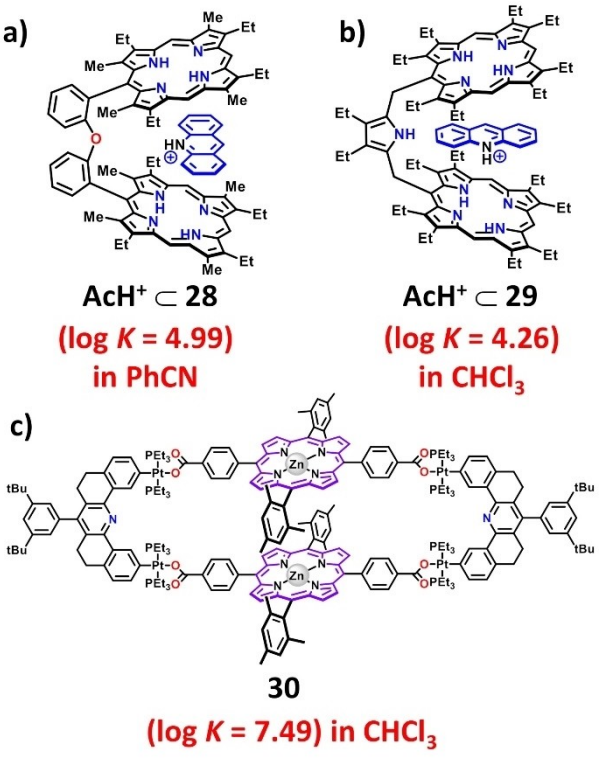

Scheme 9. Examples of some bis-porphyrin receptors interacting with protonated acridines ($\mathbf{AcH}^+$) through π-donor/π-acceptor interactions.[38c–e] Reproduced from reference [38c–e] with permission from American Chemical Society, Wiley-VCH and Elsevier.

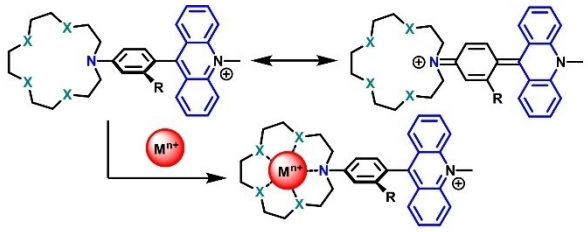

	X	R	M^{n+}	Solvent	Log *K*	Ref
31^{+}	O	H	Ca^{2+}	CH_3CN	3.06	39
			Ba^{2+}	CH_3CN	2.60	39
32^{+}	O	CH_3	Ca^{2+}	CH_3CN	3.46	41
			Ba^{2+}	CH_3CN	3.00	41
33^{+}	S	H	Fe^{3+}	CH_3CN	4.00	42
			Hg^{2+}	CH_3CN	4.62	42

Figure 11. Binding constants (log *K*) between the different macrocyclic receptors appended with acridinium units (**31**$^{+}$–**33**$^{+}$) and metal cations M^{n+} in CH_3CN at 298 K.

core.[40] Upon addition of Ca^{2+} or Ba^{2+} cations, this charge transfer band decreased and was blue-shifted (Ba^{2+} (λ_{max} = 442 nm), Ca^{2+} (λ_{max} = 428 nm)). This observation evidenced the interaction of the aniline lone pair with each cation. UV-Vis titration experiments revealed a higher affinity of the receptor for the Ca^{2+} ion (log *K* = 3.06) in comparison to the Ba^{2+} ion (log *K* = 2.60). The higher selectivity for Ca^{2+} ion was rationalized by its higher ionic character and its size ($R(Ca^{2+})$ = 1.98 Å) *vs* ($R(Ba^{2+})$ = 2.66 Å) better suited to that of the azacrown ether cavity. Based on these results, the receptor was envisaged as a selective chromoionic indicator.

Introduction of a methyl on the phenylene spacer had a minor effect on the energy of the electronic transitions of the molecule (**32**$^{+}$). However, it lowered the transition probability of the charge transfer transition.[41] Noteworthy, the binding affinity for Ca^{2+} (log *K* = 3.46) and Ba^{2+} (log *K* = 3.00) increased in comparison to the non-methylated compound. This binding difference can be rationalized by the less delocalized nitrogen lone pair thus being more available to complex the metallic cation. This hypothesis was supported by the measured torsion angle between the phenylene and the acridinium (78° for the methylated receptor in comparison to 57° in non-methylated compound) in the solid state.

More recently, T. del Giacco *et al.* have synthesized and studied an analogous system (**33**$^{+}$) incorporating an aza-thio-crown ether using steady state and time-resolved spectroscopies.[42] This modification of the macrocycle had an impressive effect on the selectivity of cations complexation as compared to the Verhoeven receptor. Indeed, binding studies of this receptor revealed a selective interaction with Hg^{2+} and Fe^{3+} ions since alkali ions (Li^{+}, Na^{+} and K^{+}), alkaline earth metals (Mg^{2+}, Ca^{2+} and Ba^{2+}) and other transition metals (Co^{2+}, Ni^{2+}, Fe^{2+}, Cu^{2+} and Zn^{2+}) did not induce absorption or emission changes up to 3×10^{-4} mol L^{-1}. This behavior can be rationalized by the high affinity of these cations for the sulfur atoms of the thio-crown ether receptor. UV-Vis titrations confirmed the hypsochromic shift of the charge transfer band in polar solvent, responsive for the solution color change from violet (550 nm) to yellow (410 nm, Figure 12a) and gave a 1:1 association event for both cations (log $K(Fe^{3+})$ = 4 and log $K(Hg^{2+})$ = 4.62 in CH_3CN). Interestingly, the binding constant between Hg^{2+} and the receptor is significantly higher in H_2O (log *K* = 5.04). Moreover, stronger fluorescence arose from the $Hg^{2+}\subset$**33**$^{+}$ complex (ϕ_F = 0.004) as compared to the free receptor (ϕ_F = 0.0011). For the free receptor, the S1 charge transfer state is non luminescent in water and the weak luminescence is assigned to the decay of S2 state localized on the methylacridinium. Complexation modified the states order (Figure 12b) and for the Hg^{2+} complex, the S1 state localized on the methylacridinium is the emitting state. Due to its high selectivity for Hg^{2+} in water, such system could be used for colorimetric and fluorimetric sensing of this harmful heavy metal ion.

4.2. Acridinium Appended to Calix[n]arenes

W. Abraham and his group have developed a family of functionalized calix[4]arene receptors with two acridinium units at their wider rim as photoswitches able to modulate the size of the cavity entrance (Figure 13a).[43] The switchable properties of these macrocycles were explored upon addition of hydroxide ions.[44] Interestingly, the conversion of the bis-acridinium macrocycle (**34**$^{2+}$) to the corresponding bis-acridane macro-

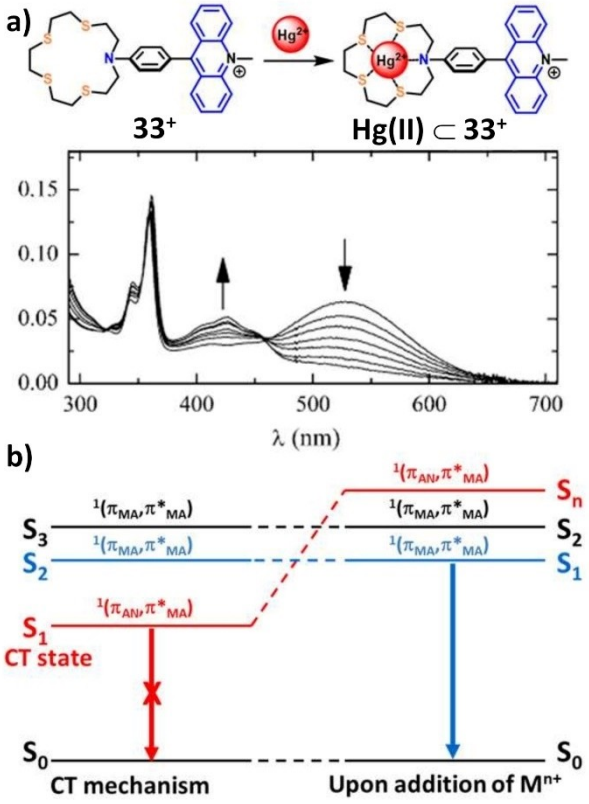

Figure 12. a) UV-Vis spectra of T. del Giacco's receptor (**33**$^{+}$) upon addition of Hg^{2+} ions in water and b) the schematized energy diagram explaining the change in absorption (AN: Aniline, MA: Methylacridinium). Reproduced from reference [42] with permission from Royal Society of Chemistry.

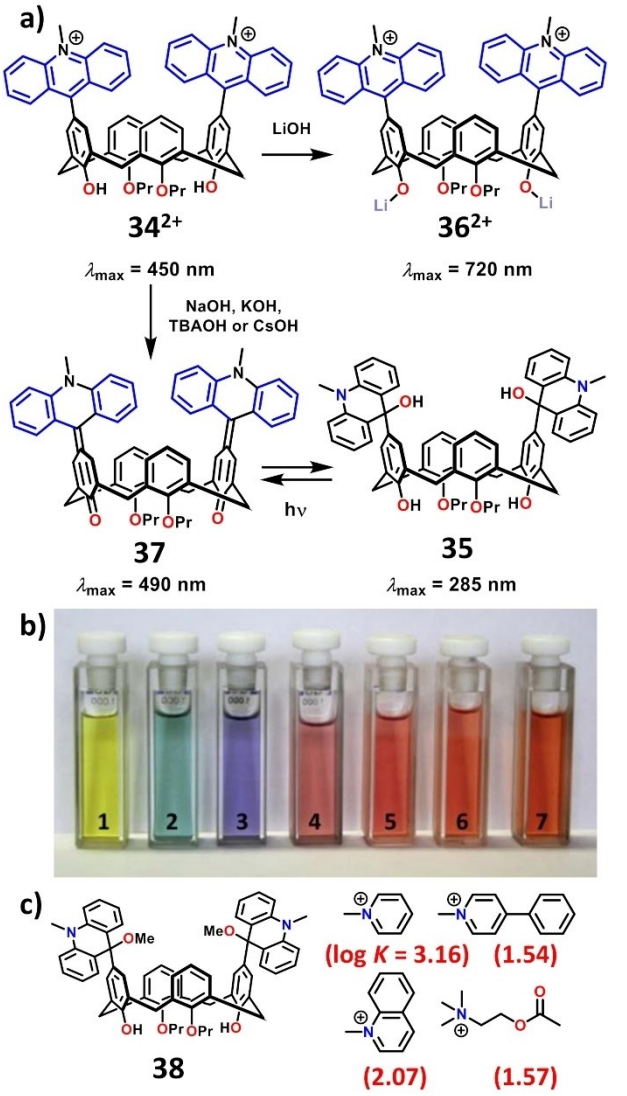

Figure 13. a) Functionalized calix[4]arene receptor with two acridinium units ($\mathbf{34}^{2+}$) able to exhibit an absorption change upon addition of hydroxide anions. b) Compound $\mathbf{34}^{2+}$ in CH_3CN ($c = 4\times10^{-5}$ mol L^{-1}) and addition of several bases ($c = 6.6\times10^{-5}$ mol L^{-1}), 1: without base, 2: LiOH, 3: NaOH, 4: KOH, 5: RbOH, 6: CsOH, 7: Et_4NOH). c) Electro-deficient guests able to interact with the bis-acridane receptor (**38**) and the corresponding binding constants (log *K*) in $CDCl_3$.[44] Reproduced from reference [44] with permission from Elsevier.

cycle (**35**) was not immediately observed in the presence of LiOH (in a H_2O/CH_3CN solvent mixture). Indeed, a color change from yellow to blue was monitored as the result of the appearance of a new electronic transition ($\lambda_{max} = 720$ nm). This color change was the result of the increased charge transfer from the phenolate to the acridinium moiety in $\mathbf{36}^{2+}$ (Figure 13b). Upon changing the cation of the base to less coordinating ions (Na^+, K^+, $(CH_3CH_2)N^+$, Cs^+), a change of the spectral properties was observed with the appearance of a new species ($\lambda_{max} = 490$ nm) attributed to the quinoid form (**37**). In all cases, slow conversion of the quinoidic calix[4]arene to the corresponding bis-acridane receptor (**35**) was achieved ($\lambda_{max} =$ 285 nm). Noteworthy, photolysis of the bis-acridane receptor **35** led to the reversible formation of the quinoid receptor. In addition, the acridane form **38** interacted with electro-deficient guests in $CDCl_3$ with moderate binding constants ($1.54 < \log K < 3.16$, Figure 13c). In contrast, the acridinium form did not show any binding event with these guests.

These macrocycles were also functionalized at the narrower rim with poly-ether chains ($\mathbf{39}^{2+}$–$\mathbf{41}^{2+}$, Figure 14).[45] Under basic conditions, the acridinium units were quantitively converted to the corresponding acridane moieties (**42**–**44**). Binding studies followed by ITC titrations revealed the capture of alkaline metals (Rb^+, Cs^+) according to the length of the polyether chain. Surprisingly, selective complexation of K^+ cation for the bis-acridane **42** or for the bis-acridinium calix[4]arene receptor $\mathbf{39}^{2+}$ was observed depending on the solvent used. Indeed in CH_3CN, the bis-acridane receptor **42** formed a 2:1 complex with K^+ ion (log $K = 6.10$) while the bis-acridinium form had no affinity. Upon addition of 20% of ethanol in CH_3CN, this tendency was totally reversed with a higher binding between the bis-acridinium host $\mathbf{39}^{2+}$ and K^+ cation (log $K =$ 4.70). In other words, the functional group at the *para* positions on the wide rim of calix[4]arene receptors and the solvent effects strongly influence the electronic density of the O atoms of the calix[4]arene moiety.

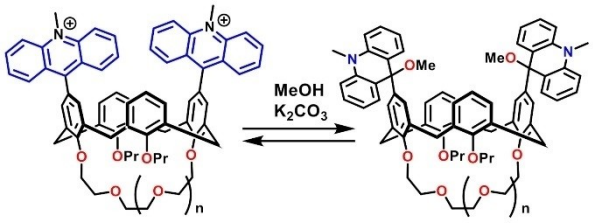

$\mathbf{39}^{2+}$, n = 2
$\mathbf{40}^{2+}$, n = 3
$\mathbf{41}^{2+}$, n = 4

42, n = 2
43, n = 3
44, n = 4

Compound	Ion	log *K*
$\mathbf{39}^{2+}$	K^+	< 2
$\mathbf{39}^{2+}$	Rb^+	< 2
$\mathbf{40}^{2+}$	K^+	< 2
$\mathbf{40}^{2+}$	Rb^+	3.29
$\mathbf{40}^{2+}$	Cs^+	4.36
$\mathbf{41}^{2+}$	Rb^+	< 2
$\mathbf{41}^{2+}$	Cs^+	< 2
42	K^+	6.10
42	Rb^+	< 2
42	Cs^+	< 2
43	K^+	< 2
43	Rb^+	4.37
43	Cs^+	5.37
44	Cs^+	3.94

Figure 14. Binding constants between the different calix[4]arene receptors ($\mathbf{39}^{2+}$–**44**) incorporating poly-ether chains and K^+, Rb^+ and Cs^+ ions in CH_3CN at 298 K.[45] Reproduced from reference [45] with permission from Elsevier.

4.3. Bis-Acridinium Tweezers

A number of molecular tweezers incorporating bis-acridinium recognition units linked by semi-rigid spacers were reported. These molecular tweezers use the electron-deficient nature of the acridinium moiety to interact with electron rich aromatic guests through π-donor/π-acceptor interactions.

An early example was described by J.-M. Lehn and co-workers in 2004.[46] In this system (**45**$^{2+}$), both acridinium recognition units are connected to a bis-pyridyl-pyrimidine spacer (Figure 15a). In the solid state the preferred conformation of this tweezer was found to be the U-shaped conformation as the result of the lone pair repulsion between the nitrogen atoms of the spacer. In this conformation, the distance between both acridinium recognition units was reported to be around 7 Å, suitable for π-donor/π-acceptor interactions. Complexation studies between this receptor and 2,3,6,7-tetrakis (dodecyloxy)anthracene led to the formation of a host-guest complex (log $K = 3.00$ in a $CDCl_3/CD_3OD$ (92:8) mixture).

More recently our group has described a family of molecular tweezers varying the spacer. A first 1,1′:3′,1″-terphenyl spacer was studied (**46**$^{2+}$, Figure 15b).[47] In the solid state, this receptor adopted a U-shaped conformation with the inclusion of a PF_6^- counter-ion inside its cavity. The distance between both acridinium moieties was found to be too high ($d = 7.804$ Å) to ensure optimum π-stacking interactions with planar electron rich aromatic guests ($d = 7.2$ Å) such as TTF and pyrene leading to low binding constants (log $K \approx 1$ in CD_3CN for both guests). However, the chemical responsive properties of this 1,1′:3′,1″-terphenyl tweezer were exploited to alter its recognition properties. Upon addition of nucleophiles (HO^-, CH_3O^-), the formed bis-acridane tweezer showed no binding affinity with both guests. The bis-acridinium receptor was restored upon addition of trifluoroacetic acid (2 eq.).

A second molecular tweezer incorporating a 2,6-diphenylpyridine spacer (**47**$^{2+}$) was developed to optimize the acridinium-acridinium distance (Figure 15c).[4] To our surprise, as shown by ^{1}H NMR experiments in CD_3CN, this tweezer exhibited a dynamic equilibrium between its monomeric form and its entwined dimer. The obtained crystal structure revealed an optimum distance between both acridinium moieties (7.138 Å) allowing π-π stacking interactions with the semi-rigid spacer of a second receptor. With chloride ions as counter ions, the tweezer was water soluble and the entwined dimer was the exclusive form detected in D_2O on account of additional hydrophobic forces. The dimerization constant was estimated to be greater than 10^5 L mol^{-1}. In a competitive solvent such as DMSO-d_6, dissociation of the dimer occurred leading to the solvation of the discrete monomer. In addition, a molecular tweezer incorporating two acridinium units bridged by a 1,3-dipyridylbenzene spacer (**48**$^{2+}$) was prepared.[48] This tweezer showed the same ability to form entwined dimers in D_2O. Interestingly, a 1:1 mixture of both 2,6-diphenylpyridine (**47**$^{2+}$) and 1,3-dipyridylbenzene tweezers (**48**$^{2+}$) showed a narcissistic self-sorting behavior with the exclusive formation of both homodimers (Figure 15c). This self-sorting behavior was found to be under thermodynamic control as the result of the difference in the binding constants between both dimer formation. DFT calculations confirmed that the homomeric dimers formation exhibited the highest driving forces ($\Delta G = -24.9$ kcal mol^{-1} and -23.0 kcal mol^{-1} respectively) compared to the heteromeric dimer ($\Delta G = -22.3$ kcal mol^{-1}).

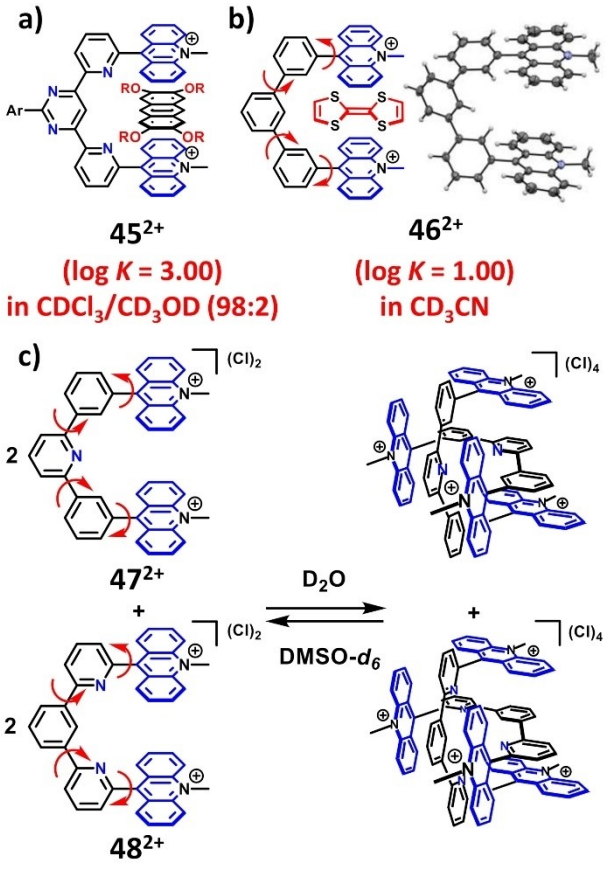

Figure 15. Bis-acridinium molecular tweezers incorporating semi-rigid spacers. a) Molecular tweezer incorporating a bis-pyridyl-pyrimidine (**45**$^{2+}$, Ar: pNBu-Ph-, R=$C_{12}H_{25}$),[46] b) a 1,1′:3′,1″-terphenyl spacer (**46**$^{2+}$) able to interact with electron rich guests and its crystal structure (PF_6 counter-ions were omitted for clarity)[47] and c) molecular tweezers showing a self-sorting behavior (**47**$^{2+}$ and **48**$^{2+}$).[4,48] Reproduced from references [4] and [47] with permission from the Royal Society of Chemistry.

4.4. Acridiniums Incorporated into Macrocycles and Cages

In 1991, J.-M. Lehn and his co-workers described a series of cyclic (**49**$^{2+}$ and **50**$^{2+}$) and acyclic bis-acridinium receptors (**51**$^{2+}$ and **52**$^{2+}$) able to bind both neutral and anionic (carboxylate, phosphate and sulfonate) aromatic substrates containing planar residues in aqueous solution (Scheme 10a).[49] Upon addition of anionic aromatic guests, 1:1 sandwich complexes were formed. As an example, macrobicyclic receptor **49**$^{2+}$ binds adenosine monophosphate (AMP^{2-}), 2,6-naphthalene dicarboxylate (2,6-NDC^{2-}), anthraquinone disulphonate ($AQDS^{2-}$), with binding constants (log $K = 3.79$, 4.59 and 5.13, respectively) lower than its acyclic analogue **51**$^{2+}$ (log $K = 4.79$, 4.75 and 5.67, Scheme 10b). The crystal structure of the cyclized receptor **49**$^{2+}$ revealed a partial occupation of the 1,4-butadiyne spacers in

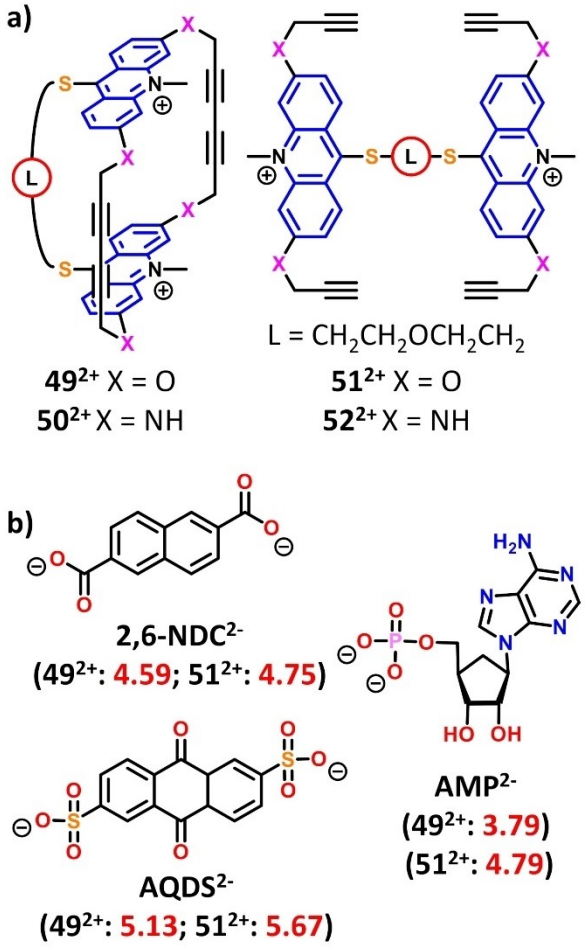

Scheme 10. a) Water soluble bis-acridinium molecular cages ($\mathbf{49}^{2+}$ and $\mathbf{50}^{2+}$) and the corresponding acyclic bis-acridinium receptors ($\mathbf{51}^{2+}$ and $\mathbf{52}^{2+}$). b) The anionic guests studied and their corresponding binding constants (log *K*) in water.[49] Reproduced from reference [49] with permission from the Royal Society of Chemistry.

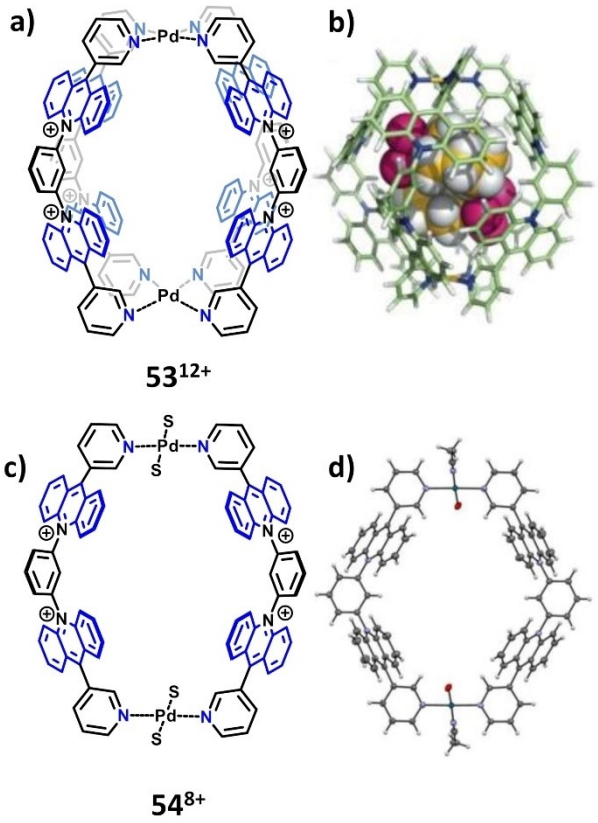

Figure 16. Scheme of a) the coordination cage ($\mathbf{53}^{12+}$) and b) its optimized structure with two encapsulated cycloheptyltrifluoroborate, c) the coordination macrocycle ($\mathbf{54}^{8+}$) and d) its corresponding crystal structure.[50] Reproduced from reference [50] with permission from Wiley-VCH.

the receptor cavity and a distance of 7.5 Å between the acridinium units (too large for optimal host-guest interactions) thus explaining these lower binding constants. Noteworthy, the cooperativity of the acridinium recognition units was confirmed by comparative titration studies with their mono-acridinium analogues showing lower binding constants of one to two orders of magnitude. As a general trend, the binding constant increases with the extension of the π-system of the guests as a result of the increase of π-surface interaction between the host and the guest. Negligible influence from the number of charges on the adenosine mono-, di- and tri-phosphate guests were found thus emphasizing the dominant role of the van der Waals and hydrophobic interactions over electrostatic forces.

M. Yoshizawa and his group were the first to report in 2016 the synthesis of a metallo-capsular based architecture with cationic aromatic panels ($\mathbf{53}^{12+}$, Figure 16a).[50] This architecture with a large cavity of 610 Å^3 was quantitatively prepared by the self-assembly of a bis-acridinium-pyridyl ligand and Pd(II) ions leading to a M_2L_4 complex. This structure was confirmed by NMR (1D and 2D) spectroscopy as well as single crystal X-ray diffraction. As the result of the twelve positive charges provided by the metal ions and acridiniums, this molecule was soluble in water as a chloride or a sulfate salt. It exhibited an unusual selective ability to capture in H_2O, alkyltrifluoroborate guest molecules (Figure 16b), namely potassium cycloheptyltrifluoroborate and cyclobutyltrifluoroborate in the presence of small anions (BF_4^-, PF_6^-, NO_3^-, SO_4^{2-}) and was unable to bind neutral guests (cyclophane, pyrene, C_{60}). For this cationic receptor, both the anionic and hydrophobic nature of the guests were critical for the stability of the host-guest complex. Noteworthy, the corresponding tubular structure M_2L_2 ($\mathbf{54}^{8+}$) was unable to form host-guest complexes with these organic trifluoroborate guests thus showing the importance of the polycationic close cavity environment (Figure 16c–d).

A year later, M. Yoshizawa and his group designed a water soluble switchable macrocycle ($\mathbf{55}^{4+}$) incorporating four acridinium units (Figure 17).[51] In an aqueous environment, this macrocycle was switched from its open to its closed conformation upon addition of hydroxide anions leading to the corresponding tetrakisacridane macrocycle (**56**). The open form was restored under acidic conditions thus showing the reversibility of the pH-dependent behavior of the macrocycle. The open-close switching cycles could be repeated several times in water. Both forms were confirmed by X-ray diffraction analysis revealing an important modification of the cavity size

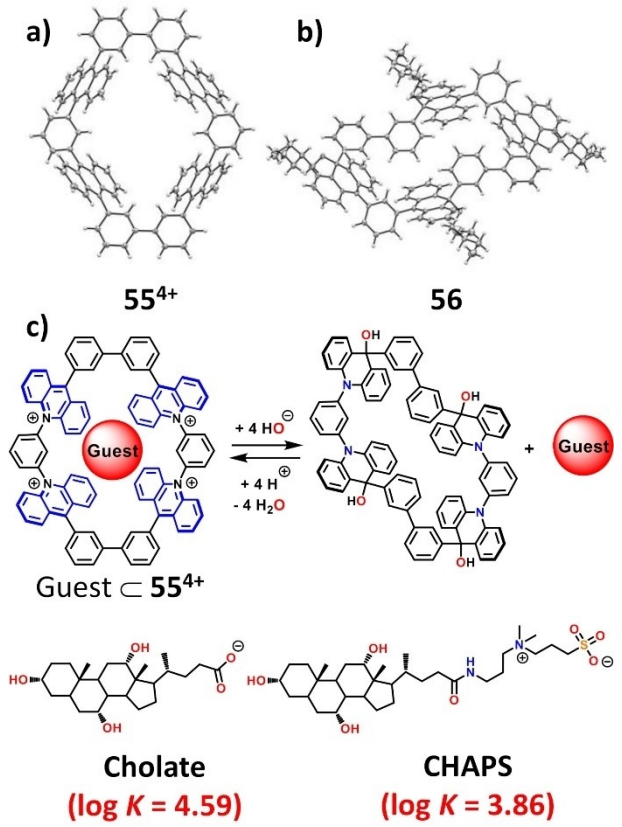

Figure 17. Crystal structures of the switchable receptor in a) its open (55^{4+}) form, b) closed form (**56**) and c) its representative scheme with the studied guests and the corresponding binding constants (log *K*) in deuterated water.[51] Reproduced from reference [51] with permission from Wiley-VCH.

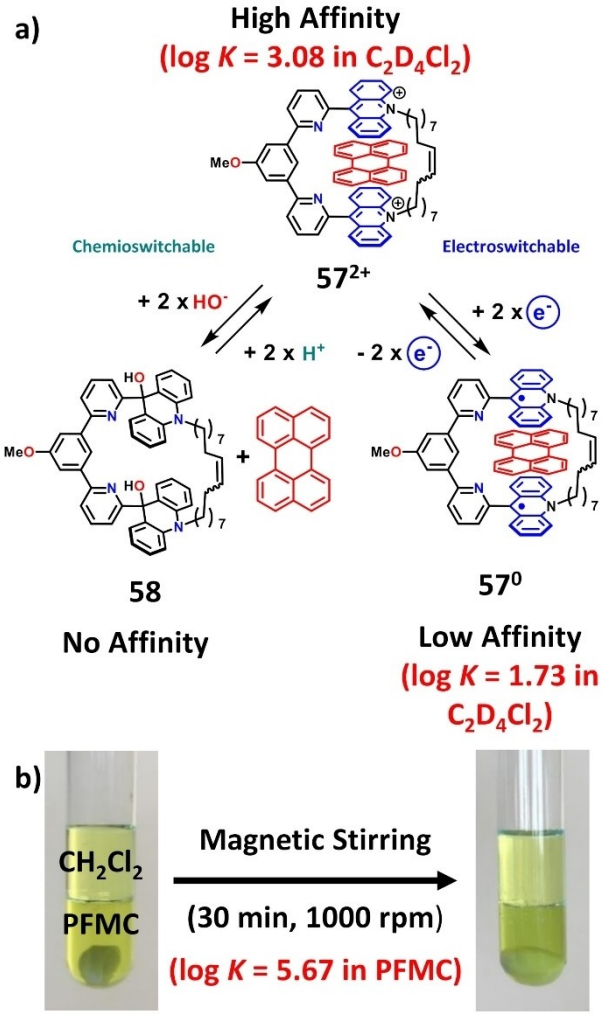

Figure 18. a) Bis-acridinium macrocycle (57^{2+}) exhibiting a high affinity with perylene. Upon chemical and electrochemical switching, the receptor releases totally or partially the guest. b) Photographs of biphasic system allowing the extraction of perylene from CH_2Cl_2 ($c = 4 \times 10^{-3}$ mol L^{-1}) to a solution of receptor 57^{2+} in PFMC ($c = 0.55 \times 10^{-3}$ mol L^{-1}, stirring bar present in the bottom of the tube).[52] Reproduced from reference [52] with permission from Wiley-VCH.

and shape (Figure 17a-b). In its open form, the cavity could host hydrophilic guests incorporating a coumarin or a steroid moiety. As revealed by ^{1}H NMR spectroscopy, a 1:2 host-guest complex was observed with esculin in which π-π stacking interactions were involved between the coumarin motif of the guest and the acridinium subunits of the macrocycle. Interestingly, steroid guests, namely sodium cholate and 3-[(3-cholamidopropyl)dimethylammonio]-1-propane sulfonate hydrate (CHAPS), exhibit a 1:1 binding event with the open macrocycle (log $K = 4.59$ and 3.86 respectively, Figure 17c). In both cases, guests were reversibly released by addition of a base leading to the precipitation of the tetrakisacridane macrocycle as the result of the disappearance of the positive charges.

Our group was also interested in synthesizing a bis-acridinium cyclophane (57^{2+}) incorporating a 3,5-dipyridylanisole spacer (Figure 18).[52] Binding studies revealed the preferential binding between this receptor and perylene (log $K = 3.08$ in $C_2D_4Cl_2$) in comparison to other polyaromatic hydrocarbons, namely anthracene and naphthalene (log $K = 1.78$ and 0.47 respectively). This complexation event led to a color change from yellow to green as the result of a partial charge transfer from perylene to the acridinium recognition units. In addition, this receptor also exhibited reversible switchable properties, chemical and electrochemical properties, allowing the release of the captured perylene (with no affinity for **58** and a log $K =$ 1.73 for 57^0 in $C_2D_4Cl_2$ Figure 18a). Finally, this macrocycle was switched from an organic to a perfluorocarbon phase, namely perfluoromethylcyclohexane (PFMC). In the PFMC phase, the macrocycle showed a much higher affinity for perylene (log $K =$ 5.67) (Figure 18b). This higher affinity in PFMC was exploited for extraction of perylene from an equimolar mixture of polyaromatic hydrocarbons in CH_2Cl_2. Thus, based on UV-Vis spectroscopy and GC analysis, the molar ratio of perylene/anthracene/naphthalene extracted and released was determined to be 9.5/1/1.05 and the recyclability of the PFMC phase was demonstrated. These results open the way to the design of related systems for purification or separation purpose of other pollutants.

5. Acridiniums in Mechanically Interlocked Molecules

The stimulus-controlled translational motion of the ring along the axis of [2]pseudorotaxanes or [2]rotaxanes is the first step to master, to access more complex molecular machines in which the motion is associated with specific functions as in natural macromolecular machines. Acridiniums as a reversible chemical/photochemical responsive unit with associated large shape changes is an attractive station to be incorporated in the wheel or the axis of interlocked molecules as shown in the following examples.

A crown-ether macrocycle incorporating an acridinium subunit (**59**$^{+}$) was synthesized by W. Abraham and coworkers (Scheme 11).[53] Its chemiochromic properties were explored and upon addition of hydroxide ions, the hydroxyacridane macrocycle (**60**) was formed. Pseudo-rotaxane formation (**61**$^{2+}$⊂**60**) between the hydroxy-acridane macrocycle (**60**) and the dipyridinium axle (**61**$^{2+}$) was monitored by ^{1}H NMR in CD_3NO_2. The host-guest complex was reported to be in a slow exchange regime on the NMR timescale and the determined binding constant was log $K = 2.2$ in deuterated nitromethane. Noteworthy, this association constant is lower than the binding constant between the axle and dibenzo[24]crown[8] macrocycle (log $K = 2.96$ in CH_3CN), also discussed by the authors, on account of steric hindrance. Moreover, no pseudo-rotaxane formation between the acridinium macrocycle and the dipyridinium axis was observed. This difference was attributed to the charge repulsion between the acridinium host (**59**$^{+}$) and the bipyridinium guest (**61**$^{2+}$). Upon irradiation at 300 nm, the dissociation of the acridane macrocycle-dipyridinium axle complex was observed as the result of the conversion of the acridane moiety into the positively charged acridinium. The [2]pseudorotaxane that consists of the dipyridinium threaded through the acridane macrocycle (**61**$^{2+}$⊂**60**) was subjected to the corresponding [2]rotaxane synthesis (Scheme 11). Functionalization of the free pyridines with two 2,4,6-triisopropylbenzene stoppers was undertaken successfully (yield 7% due to the low binding constant). In the purification process, aromatization of the acridinium moieties was performed.[54] Noteworthy, attempts to form the corresponding acridane [2]rotaxane from **62**$^{5+}$ in basic medium led to decomposition of the axis of the interlocked molecule.

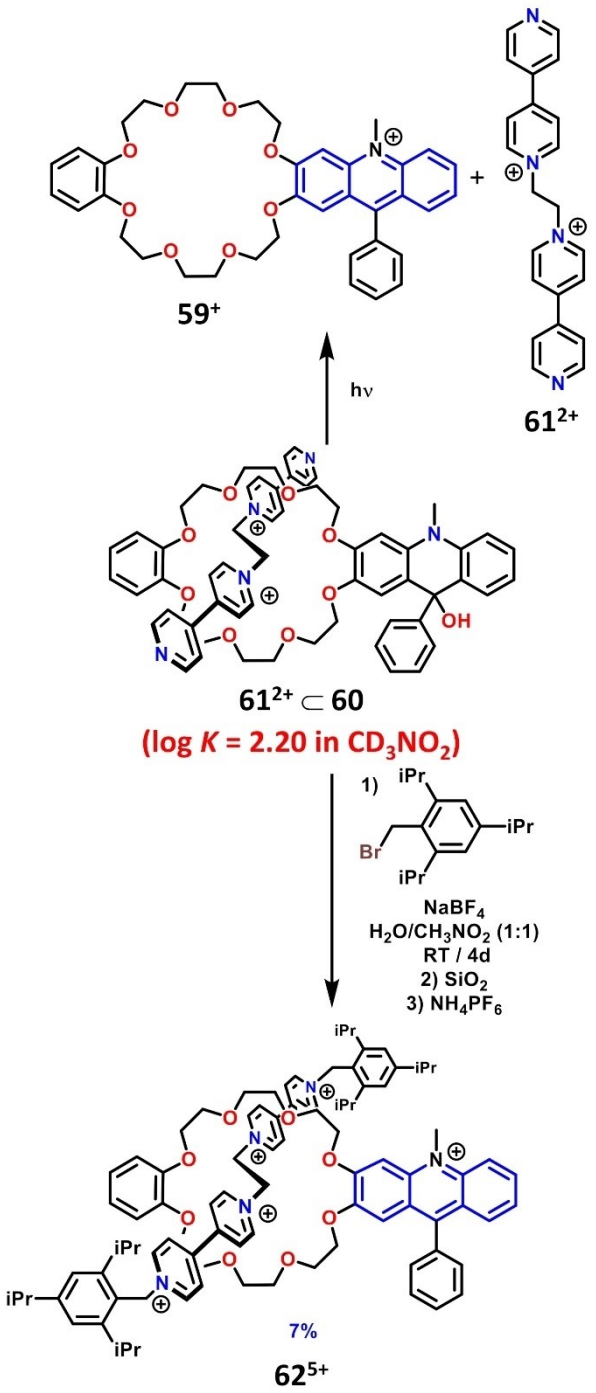

Scheme 11. Crown-ether macrocycle incorporating an acridinium moiety (**59**$^{+}$) able to form a pseudo-[2]rotaxane under its acridane form (**61**$^{2+}$⊂**60**). After a stoppering reaction, the acridinium [2]rotaxane (**62**$^{5+}$) is formed.[53,54]

The same group also reported a photoswitchable [2]rotaxane (**63**$^{5+}$) composed of a cyclobis(paraquat-*p*-phenylene) cyclophane ("bluebox") and a dissymmetric axis end-functionalized with both an acridinium and an adamantane stopper (Scheme 12).[55] From the preformed pseudo-rotaxane obtained from threading the acridane-stoppered axis through the bluebox (log $K \approx 2.74$), an esterification reaction between the terminal alcohol of the axis with the 1-adamanecarbonyl chloride afforded the [2]rotaxane. During the purification process, the acridinium stopper was obtained by aromatization under acidic conditions. In this rotaxane **63**$^{5+}$, the two identified stations were the phenoxy (B) close to the adamandate and the phenoxy (A) connected to the photoswitchable acridane/acridinum units. In its initial state, the macrocycle resides exclusively on the phenoxy station (B) of the rotaxane **63**$^{5+}$ as confirmed by ^{1}H NMR studies. Under basic conditions (K_2CO_3) in alcoholic solvents, the acridinium stopper was converted into the corresponding acridane derivative **63**$^{4+}$ initiating the movement of the macrocycle towards the acridane- phenoxy moiety. This motion was rationalized by the additional edge-to-face interaction that increased the interac-

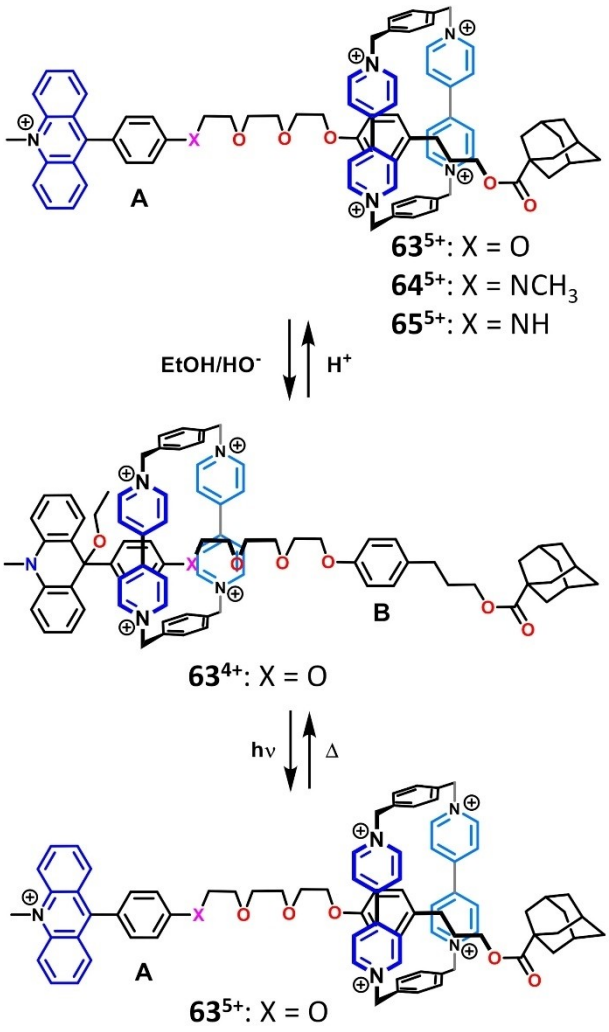

Scheme 12. Family of switchable [2]rotaxane (**63**$^{5+}$–**65**$^{5+}$) developed by W. Abraham and his coworkers incorporating a 9-aryl-acridinium stopper (station A) and a secondary station (station B).[55,56] Reproduced from references [55] and [56] with permission from the Royal Society of Chemistry.

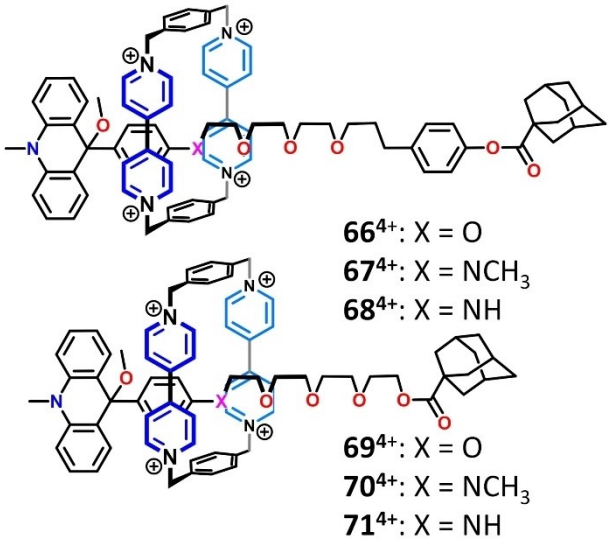

Scheme 13. Switchable [2]rotaxane (**66**$^{4+}$–**71**$^{4+}$) developed by W. Abraham and his coworkers showing no shuttling of bluebox.[56] Reproduced from reference [56] with permission from the Royal Society of Chemistry.

tion between the acridane and the tetracationic cyclophane. Upon irradiation, the acridinium stopper was recovered thus triggering the shuttling of the ring to its initial position. The back-conversion was achieved in the dark (130 s in CH_3OH). Noteworthy, the photolysis quantum yield was decreased by a factor of five in the [2]rotaxane **63**$^{4+}$ in comparison to the free axle. An analogous behavior was observed for the [2]rotaxane incorporating an aniline group (**64**$^{5+}$: N-CH_3 or **65**$^{5+}$: N–H) at the 9-position of the acridinium stopper.[56]

Noteworthy, [2]rotaxane incorporating no secondary stations (**66**$^{4+}$–**71**$^{4+}$) were also prepared (Scheme 13).[56] In this case, the ring resides exclusively on the aromatic core at the 9-aryl position of the stopper either in its acridinium or acridane form. In other words, no translational motion was observed even in the presence of a positively charged acridinium core since no other stations (even weak) are available. After irradiation, the acridane rotaxanes have a lifetime of comparable range ($70 < \tau < 220$ s) to the rotaxanes incorporating the additional phenoxy station (Scheme 12). This observation suggests that the macrocycle did not increase the steric hindrance around the 9 position of the acridinium stopper.

W. Abraham and co-workers also reported a [2]rotaxane family incorporating two acridinium stoppers (**72**$^{6+}$, **73**$^{6+}$ and **74**$^{6+}$) and secondary stations (phenoxy and/or triazole, station B) in the dumbbell (Figure 19).[57] As seen for rotaxanes with a mono-acridinium stopper (Scheme 12,13), bluebox mainly resided on the secondary phenoxy stations B or C (**72**$^{6+}$, Figure 19a). With a triazole incorporated in the thread (**73**$^{6+}$, Figure 19b), the macrocycle surrounded mainly this station. However, when a phenoxy and a triazole were present, the phenoxy mainly stabilized the ring (**74**$^{6+}$, Figure 19c). As discussed for the mono-acridane rotaxane **63**$^{4+}$ (Scheme 12), the conversion to the bis-acridane rotaxanes (e.g. in **75**$^{4+}$) increased the affinity of the ring for the stoppers and induced a large movement of the ring along the axle from one acridane station to the other one. This motion can be stopped under acidic conditions by back conversion of the acridanes to the acridiniums. This chemically-induced motion was followed by UV-vis spectroscopy with the appearance of the characteristic absorption bands at 440 nm of the acridinium units (Figure 19a). Mixed rotaxanes incorporating dissymmetric stoppers **76**$^{6+}$ revealed a preferential affinity of the tetracationic ring for the aniline station (NH > *N*-methyl, X=N station A) compared to the phenoxy station (X=O station A) on account of its steric and electronic donor abilities despite the positive charge on the nearby stopper. Photons were also used to convert both acridanes into acridinium stations. Remarkably, upon irradiation, it was demonstrated that only one of the acridane stations, the unoccupied one, underwent the photoconversion, freezing the macrocycle on the non-converted acridane of the [2]rotaxane. The photocleavage rate was faster for the free acridane in

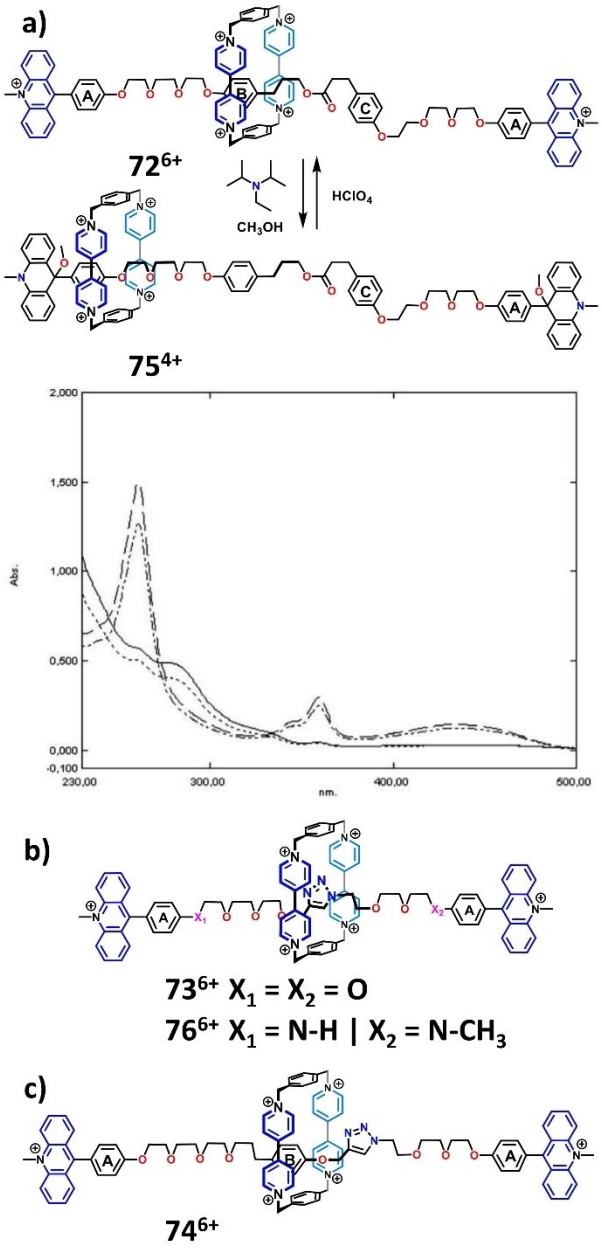

Figure 19. Family of switchable [2]rotaxane (72^{6+}–76^{6+}) developed by W. Abraham and his coworkers incorporating two 9-aryl-acridinium stoppers (station A) and secondary stations (station B).[57] a) UV/Vis spectra (CH_3CN–CH_3OH 4:1, $c = 1 \times 10^{-5}$ mol L^{-1}) of 75^{4+}, X=O before (—) and after addition of $HClO_4$ (— — —), after addition of ethyl-di-isopropylamine (– – –) and after addition of $HClO_4$ (– - - –). b) and c) Structures of the [2]-rotaxanes 73^{6+} and 74^{6+}. Reproduced from reference [57] with permission from the Royal Society of Chemistry.

comparison to the [2]rotaxane with only one acridane stopper thus increasing the photoconversion efficiency of the assembly.

Noteworthy, end-stoppered acridinium pseudorotaxanes were grafted on a gold nanoparticle surface acting as the second stopper. Remarkably, the shuttling cycles of the ring between the acridane unit and secondary phenoxy station upon photoconversion/thermal back reaction of the acridane stopper into acridinium was evidenced by UV-vis without significant fading after several cycles.[58]

6. Summary and Outlook

This review shows through many literature examples, the exploitation of N-substituted acridinium moieties as multi-recognition units in supramolecular systems. This building block is an attractive component on account of its absorption and emissive properties, reversible electrochemical reduction, reversible chemical conversion to acridane and its photochemical generation from acridane. These properties were exploited in electrochemical actuators and multi-input/multi-output systems.

The N-substituted acridinium based molecules were renowned DNA intercalators showing their ability to act as molecular guests in supramolecular systems. Consequently, this moiety was also considered as an attractive unit for molecular recognition and was encapsulated in various water-soluble hollow structures. Moreover, its positive charge was exploited to synthesize water soluble host systems thus allowing the efficient binding of electron-rich aromatic guest molecules. Finally, its intrinsic π-deficiency and switchable properties associated with geometric and electronic changes have led to its incorporation into mechanically interlocked molecules.

The unique feature of the N-substituted acridinium unit stands from its multi-input and multi-output responsiveness giving rise to various potential applications such as optical sensing, electrochemical actuation, host-guest recognition and phase transfer. Nevertheless, their potential in catalysis in confined space, self-healing material, material science, surface functionalization still remains to be explored.

Acknowledgements

This work was supported by the CNRS and the University of Strasbourg. We gratefully acknowledge the International Center for Frontier Research in Chemistry ic-FRC (www.icfrc.fr) for financial support. JH thanks the French Ministry of National Education for a PhD Fellowship.

Conflict of Interest

The authors declare no conflict of interest.

Keywords: acridinium · host-guest chemistry · multi-output units · multi-responsive units · supramolecular chemistry

[1] a) J.-M. Lehn, *Angew. Chem. Int. Ed.* **2013**, *52*, 2836–2850; b) M. W. Ambrogio, C. R. Thomas, Y.-L. Zhao, J. I. Zink, J. F. Stoddart, *Acc. Chem. Res.* **2011**, 903–913; c) B. Feringa, *Angew. Chem. Int. Ed.* **2017**, *56*, 11060–11078; d) L. van Dijk, M. J. Tilby, R. Szpera, O. A. Smith, H. A. P. Bunce, S. P. Fletcher, *Nat. Rev. Chem.* **2018**, *2*, 0117; e) A. P. DaSilva, N. D. McClenaghan, *Chem. Eur. J.* **2004**, *10*, 574–586; f) O. J. G. Goor, S. I. S. Hendrikse, P. Y. W. Dankers, E. W. Meijer, *Chem. Soc. Rev.* **2017**, *46*, 6621–6637.
[2] a) K. Gleu, A. Schubert, *Ber. Dtsch. Chem. Ges. B* **1940**, 757–761; b) B. Singer, G. Maas, *Organische Chemie* **1984**, 1399–1408.

[3] B. Zhou, K. Kano, S. Hashimoto, *Bull. Chem. Soc. Jpn.* **1988**, *61*, 1633–1640.
[4] H.-P. Jacquot de Rouville, N. Zorn, E. Leize-Wagner, V. Heitz, *Chem. Commun.* **2018**, *54*, 10966–10969.
[5] G. Jones II, M. S. Farahat, S. R. Greenfield, D. J. Gosztola, M. R. Wasielewski, *Chem. Phys. Lett.* **1994**, *229*, 40–46.
[6] S. Fukuzumi, K. Ohkubo, T. Suenobu, K. Kato, M. Fujitsuka, O. Ito, *J. Am. Chem. Soc.* **2001**, *123*, 8459–8467.
[7] a) S. Fukuzumi, H. Kotani, K. Ohkubo, S. Ogo, N. V. Tkachenko, H. Lemmetyinen, *J. Am. Chem. Soc.* **2004**, *126*, 1600–1601; b) A. C. Benniston, A. Harriman, P. Li, J. P. Rostron, H. J. van Ramesdonk, M. M. Groeneveld, H. Zhang, J. W. Verhoeven, *J. Am. Chem. Soc.* **2005**, *127*, 16054–16064; c) K. A. Margrey, D. A. Nicewicz, *Acc. Chem. Res.* **2016**, *49*, 1997–2006; d) C. A. Lawson, A. P. Dominey, G. D. Williams, J. A. Murphy, *Chem. Commun.* **2020**, *56*, 11445–11448.
[8] K. Kano, B. Zhou, S. Hashimoto, *Chem. Lett.* **1985**, 791–792.
[9] D. T. Hogan, T. C. Sutherland, *New J. Chem.* **2018**, *42*, 16469–16473.
[10] A. J. Ackmann, J. M. J. Fréchet, *Chem. Commun.* **1996**, 605–606.
[11] J. W. Bunting, V. S. F. Chew, S. B. Abhyankar, Y. Goda, *Can. J. Chem.* **1984**, *62*, 351–354.
[12] D. Zhou, R. Khatmullin, J. Walpita, N. A. Miller, H. L. Luk, S. Vyas, C. M. Hadad, K. D. Glusac, *J. Am. Chem. Soc.* **2012**, *134*, 11301–11303.
[13] Y. Xie, S. Ilic, S. Skaro, V. Maslak, K. D. Glusac, *J. Phys. Chem. A* **2017**, *121*, 448–457.
[14] Y. Hirshberg, E. Fischer, *J. Chem. Soc.* **1954**, 3129–3137.
[15] A. Raskosova, R. Stößer, W. Abraham, *Chem. Commun.* **2013**, *49*, 3964–3966.
[16] a) N. W. Koper, S. A. Jonker, J. W. Verhoeven, *Recl. Trav. Chim. Pays-Bas* **1985**, *104*, 296–301; b) C. P. Andrieux, P. Audebert, P. Hapiot, *J. Electroanal. Chem.* **1990**, *296*, 129–139; c) D. T. Hogan, T. C. Sutherland, *J. Phys. Chem. Lett.* **2018**, *9*, 2825–2829; d) P. Hapiot, J. Moiroux, J.-M. Savéant, *J. Am. Chem. Soc.* **1990**, *112*, 1337–1343.
[17] E. Ahlberg, O. Hammerich, V. D. Parker, *J. Am. Chem. Soc.* **1981**, *103*, 844–849.
[18] C.-W. Chiu, F. P. Gabbaï, *Angew. Chem. Int. Ed.* **2007**, *46*, 1723–1725.
[19] T. Suzuki, J.-I. Nishida, T. Tsuji, *Angew. Chem. Int. Ed. Engl.* **1997**, *36*, 1329–1331.
[20] T. Suzuki, A. Migita, H. Higuchi, H. Kawai, K. Fujiwara, T. Tsuji, *Tetrahedron Lett.* **2003**, *44*, 6837–6840.
[21] a) T. Suzuki, K. Wada, Y. Ishigaki, Y. Yoshimoto, E. Ohta, H. Kawai, K. Fujiwara, *Chem. Commun.* **2010**, *46*, 4100–4102; b) K. Wada, T. Takeda, H. Kawai, R. Katoono, K. Fujiwara, T. Suzuki, *Chem. Lett.* **2013**, *42*, 1194–1196.
[22] a) H. Kawai, T. Takeda, K. Fujiwara, T. Suzuki, *Tetrahedron Lett.* **2004**, *45*, 8289–8293; b) H. Kawai, T. Takeda, K. Fujiwara, M. Wakeshima, Y. Hinatsu, T. Suzuki, *Chem. Eur. J.* **2008**, *14*, 5780–5793.
[23] T. Suzuki, R. Tamaki, E. Ohta, T. Takeda, H. Kawai, K. Fujiwara, M. Kato, *Tetrahedron Lett.* **2007**, *48*, 3823–3827.
[24] T. Suzuki, K. Ohta, T. Nehira, H. Higuchi, E. Ohta, H. Kawai, K. Fujiwara, *Tetrahedron Lett.* **2008**, *49*, 772–776.
[25] Y. Sakano, R. Katoono, K. Fujiwara, T. Suzuki, *Chem. Commun.* **2015**, *51*, 14303–14305.
[26] Y. Hirao, T. Taniguchi, M. Teraoka, T. Kubo, *Asian J. Org. Chem.* **2019**, *8*, 863–866.
[27] a) X. Mei, C. Wolf, *Eur. J. Org. Chem.* **2004**, 4340–4347; b) A. Sikorski, D. Trzybiński, *Tetrahedron* **2011**, *67*, 1479–1484 ; c) L. Plasseraud, H. Cattey, *C. R. Chim.* **2013**, *16*, 613–620; d) A. Garai, S. Mukherjee, S. K. Ray, K. Biradha, *Cryst. Growth Des.* **2018**, *18*, 581–586; e) Y.-H. Peng, Z.-X. Xu, C.-H. Li, L. Hu, V. A. L. Roy, S.-F. Sun, J. Wang, *Inorg. Chim. Acta* **2014**, *410*, 88–93.
[28] a) R. V. Pereira, M. H. Gehlen, *Spectrochim. Acta Part A* **2005**, *61*, 2926–2932; b) R. V. Pereira, M. H. Gehlen, *Spectrochim. Acta Part A* **2005**, *61*, 2926–2932; c) H. Sato, M. Kawasaki, K. Kasatani, *J. Photochem.* **1981**, *17*, 243–248; d) T. Ban, K. Kasatani, M. Kawasaki, H. Sato, *Photochem. Photobiol.* **1983**, *37*, 131–139; e) S. Basili, T. Del Giacco, F. Elisei, R. Germani, *Org. Biomol. Chem.* **2014**, *12*, 6677–6683; f) T. Del Giacco, R. Germania, F. Purgatorio, M. Tiecco, *Journal of Photochemistry and Photobiology A: Chemistry* **2017**, *345*, 74–79; g) R. Germani, F. Purgatorio, P. Anastasio, L. Belpassi, F. Elisei, M. Tiecco, T. Del Giacco, *Dyes Pigm.* **2020**, *173*, 107959.
[29] a) L. S. Lerman, *J. Mol. Biol.* **1961**, *3*, 18–30; b) W. Kersten, H. Kersten, W. Szybalski, *Biochemistry* **1966**, *5*, 236–244; c) S. C. Riva, *Biochem. Biophys. Res. Commun.* **1966**, *23*, 606–611; d) H. J. Li, D. M. Crothers, *J. Mol. Biol.* **1969**, *39*, 461–477; e) H. J. Li, D. M. Crothers, *Biopolymers* **1969**, *8*, 217–235; f) E. S. Canellakis, Y. H. Shaw, W. E. Hanners, R. A. Schwartz, *Biochim. Biophys. Acta* **1976**, *418*, 277–289; g) S. C. Zimmerman, C. R. Lamberson, M. Cory, T. A. Fairley, *J. Am. Chem. Soc.* **1989**, *111*, 6805–6809; h) R. L. Jones, A. C. Lanier, R. A. Keel, W. D. Wilson, *Nucleic Acids Res.* **1980**, *8*, 1613–1624; i) C. Martins, M. Gunaratnam, J. Stuart, V. Makwana, O. Greciano, A. P. Reszka, L. R. Kelland, S. Neidle, *Bioorg. Med. Chem. Lett.* **2007**, *17*, 2293–2298.
[30] J. Joseph, E. Kuruvilla, A. T. Achuthan, D. Ramaiah, G. B. Schuster, *Bioconjugate Chem.* **2004**, *15*, 1230–1235.
[31] E. Kuruvilla, D. Ramaiah, *J. Phys. Chem. B* **2007**, *111*, 6549–6556.
[32] E. Kuruvilla, J. Joseph, D. Ramaiah, *J. Phys. Chem. B* **2005**, *109*, 21997–22002.
[33] P. Wang, Y. Yao, M. Xue, *Chem. Commun.* **2014**, *50*, 5064–5067.
[34] a) K. I. Assaf, W. M. Nau, *Chem. Soc. Rev.* **2015**, *44*, 394–418; b) S. J. Barrow, S. Kasera, M. J. Rowland, J. del Barrio, O. A. Scherman, *Chem. Rev.* **2015**, *115*, 22, 12320–12406; c) E. Masson, X. Ling, R. Joseph, L. Kyeremeh-Mensah, X. Lu, *RSC Adv.* **2012**, *2*, 1213–1247.
[35] E. Masson, Y. M. Shaker, J.-P. Masson, M. E. Kordesch, C. Yuwono, *Org. Lett.* **2011**, *13*, 3872–3875.
[36] a) F. Inokuchi, K. Araki, S. Shinkai, *Chem. Lett.* **1994**, 1383–1386; b) W. Abraham, *J. Inclusion Phenom. Macrocyclic Chem.* **2002**, *43*, 159–174.
[37] R. Frydrych, T. Lis, W. Bury, J. Cybinska, M. Stępień, *J. Am. Chem. Soc.* **2020**,*142*, 15604–15613.
[38] a) T. Mizutani, K. Wada, S. Kitagawa, *J. Am. Chem. Soc.* **2001**, *123*, 6459–6460; b) K. Wada, T. Mizutani, H. Matsuoka, S. Kitagawa, *Chem. Eur. J.* **2003**, *9*, 2368–2380; c) M. Tanaka, K. Ohkubo, C. P. Gros, R. Guilard, S. Fukuzumi, *J. Am. Chem. Soc.* **2006**, *128*, 14625–14633; d) A. Chaudhary, S. P. Rath, *Chem. Eur. J.* **2012**, *18*, 7404–7417; e) D. Kim, S. Lee, G. Gao, H. S. Kang, J. Ko, *J. Organomet. Chem.* **2010**, *695*, 111–119.
[39] S. A. Jonker, F. Ariese, J. W. Verhoeven, *Red. Trav. Chim. Pays-Bas* **1989**, *108*, 109–115.
[40] This resonance was first observed by UV-Vis by T. G. Beaumont, K. M. C. Davis, *Nature* **1970**, *225*, 632.
[41] S. A. Jonker, S. I. Van Dijk, K. Goubitz, C. A. Reiss, W. Schuddeboom, J. W. Verhoeven, *Mol. Cryst. Liq. Cryst.* **1990**, *183*, 273–282.
[42] T. del Giacco, B. Carlotti, S. De Solis, A. Barbafina, F. Elisei, *Phys. Chem. Chem. Phys.* **2011**, *13*, 2188–2195.
[43] L. Grubert, W. Abraham, *Tetrahedron* **2007**, *63*, 10778–10787.
[44] L. Grubert, H. Hennig, W. Abraham, *Tetrahedron* **2009**, *65*, 5936–5944.
[45] L. Grubert, H. Hennig, U.-W. Grummt, W. Abraham, *Tetrahedron* **2009**, *65*, 8402–8406.
[46] A. Petitjean, R. G. Khoury, N. Kyritsakas, J.-M. Lehn, *J. Am. Chem. Soc.* **2004**, *126*, 6637–6647.
[47] A. Gosset, Z. Xu, F. Maurel, L.-M. Chamoreau, S. Nowak, G. Vives, C. Perruchot, V. Heitz, H.-P. Jacquot de Rouville, *New J. Chem.* **2018**, *42*, 4728–4734.
[48] H.-P. Jacquot de Rouville, C. Gourlaouen, V. Heitz, *Dalton Trans.* **2019**, *48*, 8725–8730.
[49] S. Claude, J.-M. Lehn, F. Schmidt, J.-P. Vigneron, *J. Chem. Soc. Chem. Commun.* **1991**, 1182–1185.
[50] K. Yazaki, Y. Sei, M. Akita, M. Yoshizawa, *Chem. Eur. J.* **2016**, *22*, 17557–17561.
[51] K. Kurihara, K. Yazaki, M. Akita, M. Yoshizawa, *Angew. Chem. Int. Ed.* **2017**, *56*, 11360–11364.
[52] J. Hu, J. S. Ward, A. Chaumont, K. Rissanen, J.-M. Vincent, V. Heitz, H.-P. Jacquot de Rouville, *Angew. Chem. Int. Ed.* **2020**, DOI: 10.1002/anie.202009212.
[53] M. Orda-Zgadzaj, W. Abraham, *Synthesis* **2007**, *21*, 3345–3356.
[54] M. Orda-Zgadzaj, W. Abraham, *Tetrahedron* **2008**, *64*, 2669–2676.
[55] W. Abraham, K. Buck, M. Orda-Zgadzaj, S. Schmidt-Schäffer, U.-W. Grummt, *Chem. Commun.* **2007**, 3094–3096.
[56] W. Abraham, A. Wlosnewski, K. Buck, S. Jacob, *Org. Biomol. Chem.* **2009**, *7*, 142–154.
[57] A. Vetter, W. Abraham, *Org. Biomol. Chem.* **2010**, *8*, 4666–4681.
[58] Y. Duo, S. Jacob, W. Abraham, *Org. Biomol. Chem.* **2011**, *9*, 3549–3559.

Manuscript received: October 22, 2020
Revised manuscript received: December 18, 2020

REVIEWS

Highly versatile: N-substituted acridinium moieties are emerging building blocks in supramolecular systems on account of their unique multi-responsive properties. This Review introduces the physico-chemical properties of the N-substituted acridinium unit, and highlights some examples of the use of i) as a molecular guest, ii) as an active unit in molecular hosts, and iii) in mechanically interlocked molecules.

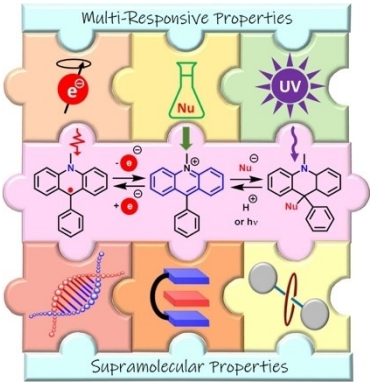

Dr. H.-P. Jacquot de Rouville, J. Hu, Prof. V. Heitz**

Review by @HPJdeRouville @Heitz_group on N-substituted acridinium as a multi-responsive recognition unit in supramolecular chemistry #ChemSupraTalents

Share your work on social media! ChemPlusChem has added Twitter as a means to promote your article. Twitter is an online microblogging service that enables its users to send and read short messages and media, known as tweets. Please check the pre-written tweet in the galley proofs for accuracy. If you, your team, or institution have a Twitter account, please include its handle @username. Please use hashtags only for the most important keywords, such as #catalysis, #nanoparticles, or #proteindesign. The ToC picture and a link to your article will be added automatically, so the tweet text must not exceed 250 characters. This tweet will be posted on the journal's Twitter account (follow us @ChemPlusChem) upon publication of your article in its final (possibly unpaginated) form. We recommend you to re-tweet it to alert more researchers about your publication, or to point it out to your institution's social media team.

ORCID (Open Researcher and Contributor ID)

Please check that the ORCID identifiers listed below are correct. We encourage all authors to provide an ORCID identifier for each coauthor. ORCID is a registry that provides researchers with a unique digital identifier. Some funding agencies recommend or even require the inclusion of ORCID IDs in all published articles, and authors should consult their funding agency guidelines for details. Registration is easy and free; for further information, see http://orcid.org/.

Johnny Hu
Dr. Henri-Pierre Jacquot de Rouville
Prof. Valérie Heitz http://orcid.org/0000-0002-5828-9199